


"In presenting the dissertation as a partial fulfillment of the requirements for an advanced degree from the Georgia Institute of Technology, I agree that the Library of the Institution shall make it available for inspection and circulation in accordance with its regulations governing materials of this type. I agree that permission to copy from, or to publish from, this dissertation may be granted by the professor under whose direction it was written, or, in his absence, by the dean of the Graduate Division when such copying or publication is solely for scholarly purposes and does not involve potential financial gain. It is understood that any copying from, or publication of, this dissertation which involves potential financial gain will not be allowed without written permission.

---



8A  
12 R-1

IONIZATION CROSS SECTIONS FOR PROTONS INCIDENT ON  
HELIUM, NEON, ARGON, HYDROGEN, NITROGEN, OXYGEN,  
AND CARBON MONOXIDE IN THE ENERGY RANGE 0.15-1.10 Mev.

A THESIS

Presented to  
the Faculty of the Graduate Division

by

John William Hooper

In Partial Fulfillment  
of the Requirements for the Degree  
Doctor of Philosophy in the School  
of Electrical Engineering

Georgia Institute of Technology

June, 1961

IONIZATION CROSS SECTIONS FOR PROTONS INCIDENT ON  
HELIUM, NEON, ARGON, HYDROGEN, NITROGEN, OXYGEN,  
AND CARBON MONOXIDE IN THE ENERGY RANGE 0.15-1.10 Mev.

Approved:

\_\_\_\_\_  
\_\_\_\_\_  
\_\_\_\_\_  
\_\_\_\_\_  
\_\_\_\_\_  
\_\_\_\_\_

Date Approved by Chairman: May 2, 1961

## DEDICATION

This thesis is gratefully  
dedicated to my wife Mary Anne  
in return for her constant  
encouragement and help.



#### ACKNOWLEDGMENTS

The successful prosecution of this work was made possible by the contributions of several people. Principal among these was Dr. E. W. McDaniel, who was the author's thesis advisor and to whom the author is greatly indebted. His guidance was invaluable in this research. Significant contributions were also made by Dr. D. W. Martin and Dr. D. S. Harmer. Dr. F. K. Hurd provided valuable suggestions in the preparation of the manuscript.

It is a pleasure to acknowledge the helpful suggestions that have been given by members of the Oak Ridge cross section group, particularly Mr. C. F. Barnett and Dr. Herman Postma. The author also expresses thanks to Mr. R. A. Langley, Mr. M. S. Spielberger, and Mr. J. W. Martin of the Engineering Experiment Station who helped to operate and repair the equipment during a portion of this work.

This research was supported by the Controlled Thermonuclear Branch of the Atomic Energy Commission under a contract administered by the Engineering Experiment Station of the Georgia Institute of Technology.

# TABLE OF CONTENTS

	Page
DEDICATION . . . . .	ii
ACKNOWLEDGEMENTS . . . . .	iii
LIST OF TABLES . . . . .	v
LIST OF ILLUSTRATIONS . . . . .	vi
SUMMARY . . . . .	viii
CHAPTER	
I. INTRODUCTION . . . . .	1
II. PHENOMENA RELATED TO THE PASSAGE OF A HOMOGENEOUS BEAM OF IONS THROUGH A GAS: COLLISION CROSS SECTIONS . . . . .	5
III. EXPERIMENTAL EQUIPMENT AND METHOD . . . . .	13
The Incident Beam Source	
The Collision Chamber	
Measurement of the Incident Beam Intensity $I_i$	
The Collector Assemblies and Electrometers	
IV. EXPERIMENTAL RESULTS . . . . .	33
Summary of Experimental Method	
Data Corrections	
Results	
Discussion of Errors	
V. COMPARISON WITH AVAILABLE THEORY . . . . .	48
Protons Incident on Molecular Hydrogen	
Protons Incident on Helium	
Comparison of Experimental Cross Sections Obtained for Incident Protons and Electrons of Equal Velocity	
VI. CONCLUSIONS . . . . .	65
APPENDIX	
THE CONCEPT OF THE COLLISION CROSS SECTION . . . . .	68
BIBLIOGRAPHY . . . . .	72
VITA . . . . .	74

## LIST OF TABLES

Table		Page
1	Calculated Values for the Equation $\sigma_i = A \times E^{-C}$ cm <sup>2</sup> /molecule . . . . .	46

## LIST OF ILLUSTRATIONS

Figure		Page
1.	Schematic View of Apparatus for Gross Ionization Measurements . . . . .	14
2.	Interior View of the Collision Chamber . . . . .	17
3.	Incident Beam Collected in Faraday Cup versus Suppression Voltage . . . . .	21
4.	Single Electrode Structure . . . . .	23
5.	Apparent Ion Currents versus Suppressor Grid Voltage for Constant Collection Field . . . . .	26
6.	Observed Ionization Cross Section for Various Collection Field Strengths . . . . .	28
7.	Leakage Currents versus Collection Voltage . . . . .	31
8.	Impurity Contributions for Protons Incident on Background Gas . . . . .	35
9.	Computed Ionization Cross Section for Varying Target Gas Pressure . . . . .	37
10.	Gross Ionization Cross Section for Protons Incident on Helium . . . . .	38
11.	Gross Ionization Cross Section for Protons Incident on Neon . . . . .	39
12.	Gross Ionization Cross Section for Protons Incident on Argon . . . . .	40
13.	Gross Ionization Cross Section for Protons Incident on Molecular Hydrogen . . . . .	41
14.	Gross Ionization Cross Section for Protons Incident on Molecular Nitrogen . . . . .	42
15.	Gross Ionization Cross Section for Protons Incident on Molecular Oxygen . . . . .	43
16.	Gross Ionization Cross Section for Protons Incident on Carbon Monoxide . . . . .	44

Figure		Page
17.	Comparison of the Experimental and Theoretical Gross Ionization Cross Sections for Protons Incident on Molecular Hydrogen . . . . .	52
18.	Comparison of the Experimental and Theoretical Gross Ionization Cross Sections for Protons Incident on Helium .	54
19.	Comparison of Experimental Gross Ionization Cross Sections for Protons and Electrons of Equal Velocity Incident on Helium . . . . .	56
20.	Comparison of Experimental Gross Ionization Cross Sections for Protons and Electrons of Equal Velocity Incident on Neon . . . . .	57
21.	Comparison of Experimental Gross Ionization Cross Sections for Protons and Electrons of Equal Velocity Incident on Argon . . . . .	58
22.	Comparison of Experimental Gross Ionization Cross Sections for Protons and Electrons of Equal Velocity Incident on Molecular Hydrogen . . . . .	59
23.	Comparison of Experimental Gross Ionization Cross Sections for Protons and Electrons of Equal Velocity Incident on Molecular Nitrogen . . . . .	60
24.	Comparison of Experimental Gross Ionization Cross Sections for Protons and Electrons of Equal Velocity Incident on Molecular Oxygen . . . . .	61
25.	Comparison of Experimental Gross Ionization Cross Sections for Protons and Electrons of Equal Velocity Incident on Carbon Monoxide . . . . .	62
26.	Gross Ionization Cross Sections for Protons Incident on Helium, Neon, Argon, Molecular Hydrogen, Molecular Nitrogen, Molecular Oxygen, and Carbon Monoxide . . . . .	66



## SUMMARY

The gross ionization cross sections for protons incident on helium, neon, argon, hydrogen, nitrogen, oxygen, and carbon monoxide have been measured for incident particle energies over the range from 0.15 to 1.10 Mev. Previous measurements by other investigators in this field have been confined to incident particle energies below 0.18 Mev.<sup>6,7,12,14,15,16</sup> The work reported here represents an extension into a region that is largely unexplored.

The atomic and molecular reactions, in addition to simple dissociation and/or excitation, that can occur when fast atoms or atomic ions collide with the molecules of a target gas may be conveniently classed as either "ionization" or "charge transfer" events. There is no general agreement on the exact definition of these terms--here it is chosen to define them as follows: In an "ionization" event, the fast particle ionizes the struck molecule but emerges with no change in its own charge state, while in a "charge transfer" event the fast particle either gains one or more electrons from, or loses one or more electrons to, the target particle. For a given projectile on a given target, each class of events in general includes several distinct kinds of reactions differing in the array of slow residual particles that are produced. The energies of the latter are usually low, although a small fraction of them may have energies as high as a few hundred electron volts. In either ionization or charge transfer, the incident particle almost always suffers only a small loss of energy and emerges with only a slight deviation from its original direction of motion.

For these ionization experiments, the source of energetic protons was a 1-Mev Van de Graaff positive ion accelerator, which was equipped with a beam analyzing and stabilizing system. The beam was passed through collimating apertures and into a collision chamber containing the target gas. The chamber dimensions and gas pressure were such that the target was "thin," in the sense that only a small fraction of the incident particles underwent any collisions at all. Electrodes parallel to the beam axis in the collision chamber collected the slow charged residual particles produced in ionizing collisions, while the original incident particles passed through the collision volume and into a Faraday cup. Detection of both the slow and fast particles was accomplished by electrometer measurements of the electron and ion currents. A complete discussion of the design considerations and the detailed testing of the apparatus is given in Chapter III. Particular attention was paid to scattering of the incident beam from apertures, Faraday cup design for proper measurement of the incident beam current, the effect of background contributions and their proper assessment, target gas pressure determination, the suppression of secondary emission from collection electrode structures, collection volume definition, collection efficiency, the effects of leakage currents, and the assessment of charge transfer contributions.

Values for the absolute gross ionization cross sections for protons incident on helium, neon, argon, hydrogen, nitrogen, oxygen, and carbon monoxide are presented along with the data of other investigators which are available in the lower energy range. It is shown that there is considerable disagreement in the low energy range among some of the

results; however, the values of Afrosimov, et al.<sup>6</sup>, for protons in hydrogen, and Fedorenko, et al.<sup>7</sup>, for protons in neon and helium agree with the present results quite satisfactorily in the region between 0.15 and 0.18 Mev that overlaps the present results.

By far the greatest uncertainty in the present experiments lay in the determination of the target gas pressure. Use of a cathetometer was believed to permit a relative reading accuracy of the McLeod gauge of less than 1 per cent. This gauge had not been absolutely calibrated, however, so a possible error of about  $\pm 5$  per cent must be admitted in the absolute reading. This led to a proportionate possible systematic error in the absolute magnitude of the cross sections. Other error contributions led to a gross possible error of  $\pm 6$  per cent in the absolute normalization of the cross section curves. The slopes of the curves are shown to be less uncertain than the cross section magnitudes.

The results gave an excellent fit to a straight line on a log-log plot throughout the energy range for all cases examined except carbon monoxide. The carbon monoxide data also fit a straight line for energies greater than approximately 0.4 Mev. The data therefore correspond, with the noted exception, to an expression of the form:

$$\sigma_i = A \times E^{-C} \text{ cm}^2/\text{molecule}$$

where E represents the incident particle energy. A Burroughs 220 electronic computer was programmed to compute the values A and C which corresponded to a least-squares fit to the average cross sections obtained from many individual runs, and to compute the probable errors in these constants that are indicated by the scatter of the data. The resulting



values are presented in Table 1, Chapter IV. The probable error of the normalization constant A that was computed from the scatter of the data was shown to be less than 1 per cent in all cases. The previously mentioned possible error of about  $\pm 5$  per cent caused by the uncertainty in the target gas pressure does not appear in these computed values since such an error is systematic.

It is emphasized that the relative values of the cross sections at various energies are not subject to this systematic error, and the uncertainties in the slopes of the lines are as indicated by the probable errors of the constant C in Table 1. Furthermore, the relative magnitudes of the cross sections for the various gases at a given energy are uncertain by no more than about  $\pm 2$  per cent.

The result for protons incident on molecular hydrogen is in excellent agreement with an approximate extension to the molecular case of a Born approximation calculation<sup>1</sup> of the cross section for the atomic process  $H^+ + H^0 \rightarrow H^+ + H^+ + e$ . The scaling procedure is discussed in Chapter V. It is demonstrated that at high energies there is essentially perfect agreement between the theoretical cross sections obtained from this scaling operation and the experimental values, within the previously stated experimental uncertainties.

Theoretical calculations in the Born approximation of the cross sections for ionization and simultaneous ionization and excitation of helium by protons have been made by Mapleton.<sup>2</sup> He assumed that the helium wave functions may be approximated by products of normalized hydrogen wave functions in which the helium nucleus had an effective charge  $Z_1$  of 1.6875 for the ground state. Mapleton examined three cases corresponding to

various choices for  $Z_2$  the effective charge associated with the Coulomb field acting on the final state bound electron, and  $Z_3$  the effective charge associated with the Coulomb field acting on the final state positive energy electron. There is essentially perfect agreement within the stated experimental uncertainties between the theoretical calculation and the experimental results in the energy range above approximately 400 kev.

Further corroboration of the present experimental results for incident protons comes from a comparison of the scaled cross sections for  $\alpha$ -particles incident on helium which have been calculated by Erskine.<sup>17</sup> Mapleton has demonstrated that translation of Erskine's results to the proton case leads to close agreement with his Case III.

It has been pointed out by Mott and Massey<sup>19</sup>, Bates and Griffing<sup>1</sup>, Mapleton<sup>2</sup>, and others that if the velocities of relative motion are the same, and are sufficiently high, the ionization cross sections for electron-atom and proton-atom collisions calculated in the Born approximation are the same. The velocity of relative motion is the same in both the laboratory and the center-of-mass coordinate systems. It is possible therefore to translate the electron cross section data by multiplying the electron energy scale by the ratio of the proton to the electron mass.

It is demonstrated that there is excellent agreement between the cross sections obtained with incident electrons<sup>18,20,21,22,23,24,25,26</sup> and with incident protons of the same velocity for the target gases helium, neon, argon, nitrogen, oxygen, and carbon monoxide. Excellent

agreement is also obtained for the molecular hydrogen case if only the data of Tate and Smith<sup>20</sup>, Bleakney<sup>23</sup>, and Tozer and Craggs<sup>22</sup> are considered.

The available electron data<sup>20</sup> indicate that the cross sections for nitrogen and carbon monoxide are equal at high energies. It was found that the proton results are unequal by about 12 per cent. Despite the fact that the electron results lie between the proton results for the two gases and are within the limits of the stated experimental uncertainties for the proton measurements on both gases, it does not seem likely that the proton experimental errors could be such as to lead to the observed displacement of the curves, since, as it was pointed out earlier, the experimental error is believed to be largely systematic and attributable to inaccuracy in the McLeod gauge calibration.

The composite results indicate that it is justifiable to scale electron cross sections to proton cross sections for the gases investigated under the assumed high velocity conditions.

## CHAPTER I

### INTRODUCTION

The ionization produced by the passage of ions and atoms through gases has been the subject of many investigations, but practically all of the experimental work done to date in this field has been confined to energies below 180 kev. The work reported here therefore represents an extension into a region that is largely unexplored.

The phenomenon of ionization of gases by fast particles is of basic theoretical interest and has considerable importance from the practical standpoint as well. In the field of controlled thermonuclear reactions there are several fusion devices which utilize high energy injection, and knowledge of the ionization cross sections for various projectiles moving at high velocities through various target gases should prove of real value. Not only are hydrogen and helium targets of interest in this connection-- heavier gases, such as carbon monoxide, may also be important since they are present in fusion devices as contaminants.

Detection of fast charged particles in gas-filled counters and cloud chambers depends directly on the ionization produced by the primary particles, and the detection of neutrons in  $\text{BF}_3$  and proton-recoil counters and in fission chambers involves the production of ion-pairs following a nuclear reaction in the target material. Another problem of interest in nuclear physics which involves the production of ion-pairs in gases is that of the design of high current ion sources for use in accelerators.



Ionization cross sections at high energies enter into consideration in a number of astrophysical and upper atmospheric phenomena related to communications. The use of ion guns for space propulsion is also under consideration.

Comparison between experimental and theoretical cross sections for high-energy ionization is desirable. Such comparison can provide checks on the various approximations to which recourse must be made in the application of atomic collision theory to the ionization problem. At the present time theoretical results are available for atomic hydrogen<sup>1</sup>, helium<sup>2</sup>, and lithium<sup>3</sup> and it seems certain that other cases will be investigated within the next few years.

The atomic and molecular reactions that can occur when fast atoms or atomic ions collide with the molecules of a target gas may be conveniently classed as either "ionization" or "charge transfer" events. There is no general agreement on the exact definition of these terms--here it is chosen to define them as follows: in an "ionization" event, the fast particle ionizes the struck molecule but emerges with no change in its own charge state, while in a "charge transfer" event the fast particle either gains one or more electrons from, or loses one or more electrons to, the target particle. For a given projectile on a given target, each class of events in general includes several distinct kinds of reactions differing in the array of slow residual particles that are produced. The energies of the latter are usually low, although a small fraction of them may have energies as high as a few hundred electron volts. In either ionization or charge transfer, the incident particle almost always suffers only a small loss of energy and emerges with only a slight deviation from its original direction of motion.

In charge transfer studies, the sum of the cross sections for all types of events that produce a given change in the charge state of the fast particle may be measured by observing the distribution of charge states in the emerging fast beam. Such measurements have been made previously for hydrogen atoms and ions incident on helium, argon, hydrogen, and nitrogen gases with energies up to 1.0 Mev.<sup>4</sup> The observed cross sections indicated that in the energy range of this research charge transfer should not make a significant contribution. Experimental results bore out this expectation.

To study ionization events one must collect and observe the slow charged particles produced by the collisions, since the emerging fast beam contains no information about the occurrence of these events. To avoid confusion due to multiple reactions by a single incident particle, the target must be "thin" in the sense that most of the incident particles will traverse the target with no collisions at all.

The experimental work done on ionization by fast ions and atoms prior to 1951 has been thoroughly surveyed by Massey and Burhop.<sup>5</sup> Most of the experiments, both before and since 1951, have been confined to energies below 40 kev. Some recent Russian work and the work reported herein are exceptions to this statement: Afrosimov, et al.<sup>6</sup>, have measured the cross section for ionization produced by protons in hydrogen from 0.005-0.18 Mev. Fedorenko, et al.<sup>7</sup>, have performed similar measurements for protons in helium, neon, and argon. The cross sections for ionization of helium, neon, argon, hydrogen, nitrogen, oxygen, and carbon monoxide in the energy range 0.15-1.10 Mev were the subject of this research.

The most recent reviews of the charge transfer field appear to be those of Allison.<sup>8,9</sup> Allison's articles concentrate on investigations of charge-changing collisions of hydrogen and helium ions and atoms at kinetic energies above 0.2 kev. He discusses all of the previous charge-changing work which has an important bearing on this research. Hasted<sup>10</sup> has reviewed the experimental techniques applied to the study of inelastic collisions between atomic systems and presents some limited results. He makes a comparison of experiment and theory wherever possible.

## CHAPTER II

### PHENOMENA RELATED TO THE PASSAGE OF A HOMOGENEOUS BEAM OF IONS THROUGH A GAS: THE CONCEPT OF COLLISION CROSS SECTION

The passage of a homogeneous beam of fast ions or atoms through a gas leads to both elastic and inelastic collisions between the incident and target particles. An elastic collision may be defined as one in which there is no change in the energies of the internal motions of the target particle or the incident projectile and in which the kinetic energy of the system is conserved. A transfer of kinetic energy usually does occur. The inelastic collision, on the other hand, results in a transformation of kinetic energy into internal energy, or vice versa, of either the struck particle or the projectile or both. This transfer of energy results in the excitation of internal motion in the particle receiving the energy or in an increase in its kinetic energy. The concept of inelastic collisions may be expanded to include the radiative effects due to Bremsstrahlung. An inelastic collision of a type sometimes referred to as "superelastic" arises from a collision between an excited structure and an incident projectile leading to de-excitation of the structure without radiation.

One possible subdivision of inelastic collisions would be as follows:

- |                |                     |
|----------------|---------------------|
| (a) radiation  | (d) charge transfer |
| (b) excitation | (e) dissociation    |
| (c) ionization |                     |



Radiation results from an inelastic collision in which some of the kinetic energy of the incident projectile enters the radiation field rather than entering into a change in the internal motion of either the projectile or target particle. This radiation, which is frequently called Bremsstrahlung, may be classically considered to arise from the acceleration of the charged particle in the atomic field of the target atoms. The effect, whose magnitude is inversely proportional to the square of the mass of the projectile, is essentially negligible when dealing with heavy particles such as ions in the energy range of this research.

Excitation may be considered as a change in atomic state of one or more of the electrons associated with the particle receiving the potential energy, or in a change in the vibrational or rotational states of the system. A change in the potential energy sufficient to lead to the ejection of one or more electrons is excluded from the excitation classification but instead is considered to be ionization. The transfer of one or more electrons between the struck particle and the projectile is classified as charge transfer. Dissociation results as a consequence of the formation of unstable molecular structures. It is possible to have combinations of any of the preceding events.

To illustrate the multiplicity of possible reactions, a list of the possible reactions for the case of fast protons incident on molecular hydrogen is presented below. The first symbol appearing on the right-hand side of each equation denotes the projectile particle after the collision. This particle may or may not have experienced a change in its charge state as the result of the reaction, but in any event theory and experiment show that it retains essentially all of its initial energy and its original direction of motion.



Reactions (1-4) are charge transfer events whereas reactions (5-8) represent ionization. Dissociation also occurs in several of these events. Reaction (9) which yields two slow hydrogen atoms is unobservable in any experiment involving the collection of charged particles and is therefore omitted from the following discussion. As an example of the interpretation of the preceding equations consider reaction (1) in which a fast  $\text{H}^+$  ion is incident on an  $\text{H}_2^{\circ}$  gas molecule. Two electrons are transferred to the incident particle and the resulting  $\text{H}_2^{++}$  gas ion, which is unstable since it consists of two positively charged particles, dissociates into two slow  $\text{H}^+$  ions.

Ionization and charge transfer measurements pertaining to reactions of the type listed above may be divided into two major categories. These are:

- (a) The "thick" target approach in which the incident particle beam passes through a sufficient quantity of target material to attain a statistical charge-state equilibrium. This method has been utilized by Allison<sup>8</sup>, Stier and Barnett<sup>11</sup>, and many others.
- (b) The "thin" target approach, in which the probability of multiple collisions by a single incident ion or atom is negligible. This method has been described by Keene<sup>12</sup>, Hasted and his collaborators<sup>13,14</sup>, and by Barnett and Reynolds.<sup>4</sup>

Method (b) lends itself to a further subdivision on the basis of particle measurement techniques. It is possible to perform an analysis of the beam constituents after passage through the target gas as done in the thick target approach. It is further possible to analyze the products of collision by applying a transverse collection field to the collision chamber. In some cases this added source of information provides the means for the subdivision of the results of the gross measurements into results pertaining to individual reactions.

It is well known that in microscopic physics, theory will not in general predict certainties but instead will yield only probabilities. This is true for collision processes of all kinds. It is therefore necessary to develop a means of expressing the probability that some particular event will occur. The concept of collision cross section, which is developed mathematically in Appendix I, is frequently used when quantitatively discussing such probabilities. This concept permits the assignment of a hypothetical size, which is related to the probability of

occurrence of a specific event, to the target particles. It is important to note that this "size" has no direct relation to the physical dimensions of the atoms or ions under consideration.

Reaction equations (1-9) illustrate the multiplicity of events which may result from the passage of a beam of ions through a gas. Slow secondary ions in the target gas are seen to result from charge exchange, from ionization of the hydrogen molecules without dissociation, and from dissociation of the molecules after ionization or charge transfer has occurred. This same information can be presented in terms of cross sections in the following manner. Let  $\sigma_{ab}^{mn}$  represent the cross section for a reaction of unspecified type. Adopting an expanded version of Hasted's notation<sup>10</sup> we let the subscripts a and b, which precede the cross section symbol, represent the initial charge states of the incident projectile and target molecule, respectively. m represents the final charge state of the incident projectile and n denotes the net positive charge associated with the residual gas ions. The net number of electrons and/or negative ions present in the gas can be obtained from a consideration of net charge equality prior to and after the collision. The superscript c, i, or d indicates reference to the specific case of charge transfer, ionization, or dissociation, respectively. Compound superscripts are provided to account for reactions in which several of the basic processes occur simultaneously. The multiple reactions may now be represented by the cross sections of equations (1'-9').

$$10 \sigma_{12}^{ccd} \quad (1')$$

$$10 \sigma_{01}^c \quad (2')$$



$$10^{\sigma_{02}^{cid}} \quad (3')$$

$$10^{\sigma_{01}^{cd}} \quad (4')$$

$$10^{\sigma_{11}^i} \quad (5')$$

$$10^{\sigma_{11}^{id}} \quad (6')$$

$$10^{\sigma_{12}^{iid}} \quad (7')$$

$$10^{\sigma_{11}^{idc}} \quad (8')$$

$$10^{\sigma_{10}^d} \quad (9')$$

Let  $\sigma_i^+$  represent the total cross section for the production of slow positive ions and  $\sigma_i^-$  represent the total cross section for the production of free electrons and negative ions. In a "thin" target experiment these cross sections are calculated from the relations

$$\sigma_i^+ = (I^+/I_i)(1/n\ell) \text{ cm}^2/\text{molecule} \quad (10)$$

$$\sigma_i^- = (I^-/I_i)(1/n\ell) \text{ cm}^2/\text{molecule} \quad (11)$$

where  $I^+$  and  $I^-$  are the positive and negative currents collected from a collision region of length  $\ell$  by transverse electric fields,  $n$  is the number density of gas molecules in the collision chamber, and  $I_i$  is the incident ion current. These expressions are developed in Appendix I.

It is evident that  $\sigma_i^+$  and  $\sigma_i^-$  can be represented in terms of the individual cross sections (1'-9') as follows:

$$\begin{aligned}\sigma_i^+ = & [10\sigma_{01}^c + 10\sigma_{01}^{cd} + 10\sigma_{11}^i + 10\sigma_{11}^{id} + 10\sigma_{11}^{idc}] \\ & + 2[10\sigma_{12}^{ccd} + 10\sigma_{02}^{cid} + 10\sigma_{12}^{iid}] \text{ cm}^2/\text{molecule}\end{aligned}\quad (12)$$

$$\begin{aligned}\sigma_i^- = & [10\sigma_{02}^{cid} + 10\sigma_{11}^i + 10\sigma_{11}^{id} + 10\sigma_{11}^{idc}] \\ & + 2[10\sigma_{12}^{iid}] \text{ cm}^2/\text{molecule}\end{aligned}\quad (13)$$

These expressions clearly demonstrate that a measurement involving the collection of only the gross positive and negative charges arising in the collision volume will lead to an unequal weighting of individual events. Further information must be obtained if separation of the individual cross sections is to be realized.

Some insight into the significance of this unequal weighting can be obtained by considering the difference in  $\sigma_i^+$  and  $\sigma_i^-$ .

$$\sigma_i^+ - \sigma_i^- = [10\sigma_{02}^{cid} + 10\sigma_{01}^c + 10\sigma_{01}^{cd}] + 2[10\sigma_{12}^{ccd}] \quad (14)$$

The cross section  $10\sigma_{12}^{ccd}$  has been shown to be very small at energies above 0.04 Mev.<sup>8</sup> For the gases studied in the present research the positive and negative currents measured at the collection plates were equal, within the limits of experimental error, for normal operation throughout the energy range 0.15-1.10 Mev. This implies that the sum of the cross sections  $10\sigma_{02}^{cid}$ ,  $10\sigma_{01}^c$ , and  $10\sigma_{01}^{cd}$  is negligible in equation (12). Therefore a measurement of the gross positive ion current for incident proton energies greater than 0.15 Mev yields in effect the cross section

$$\sigma_i = {}_{10}\sigma_{11}^i + {}_{10}\sigma_{11}^{id} + {}_{10}\sigma_{11}^{idc} + 2({}_{10}\sigma_{12}^{iid}) \quad (15)$$

where

$$\sigma_i = \sigma_i^+ \approx \sigma_i^-$$

There is reason to believe that  ${}_{10}\sigma_{11}^{idc}$  is negligible due to the relative complexity of the event, however, this fact has not been definitely established.

Experimental values for  $\sigma_i$  for protons in the energy range 0.15-1.10 Mev incident on helium, neon, argon, hydrogen, nitrogen, oxygen, and carbon monoxide gases are presented in Chapter IV.

### CHAPTER III

#### EXPERIMENTAL EQUIPMENT AND METHOD

The objective of this research was the measurement of the ionization cross section for protons incident on helium, neon, argon, hydrogen, nitrogen, oxygen, and carbon monoxide. The energy of the incident particles ranged from 0.15-1.10 Mev.

The source of the energetic protons was a 1-Mev Van de Graaff positive ion accelerator, which was equipped with a beam analyzing and stabilizing system. The beam was passed through collimating apertures and into a collision chamber containing the target gas. The chamber dimensions and gas pressure were such that the target was "thin," in the sense that only a small fraction of the incident particles underwent any collisions at all. Electrodes parallel to the beam axis in the collision chamber collected the slow charged particles produced in ionizing collisions, while the original incident particles passed through the collision volume and into a Faraday cup. Detection of both the slow and fast particles was accomplished by electrometer measurements of the electron and ion currents.

A schematic drawing of the apparatus is given in Figure 1, which includes a number of the most relevant dimensions. Following is a point by point discussion of the more important features of the apparatus, considered in sequence from the ion source to the electrometer circuits.

The Incident Beam Source.---Prior to entering the apparatus at the right side of Figure 1, the beam from the Van de Graaff was first deflected



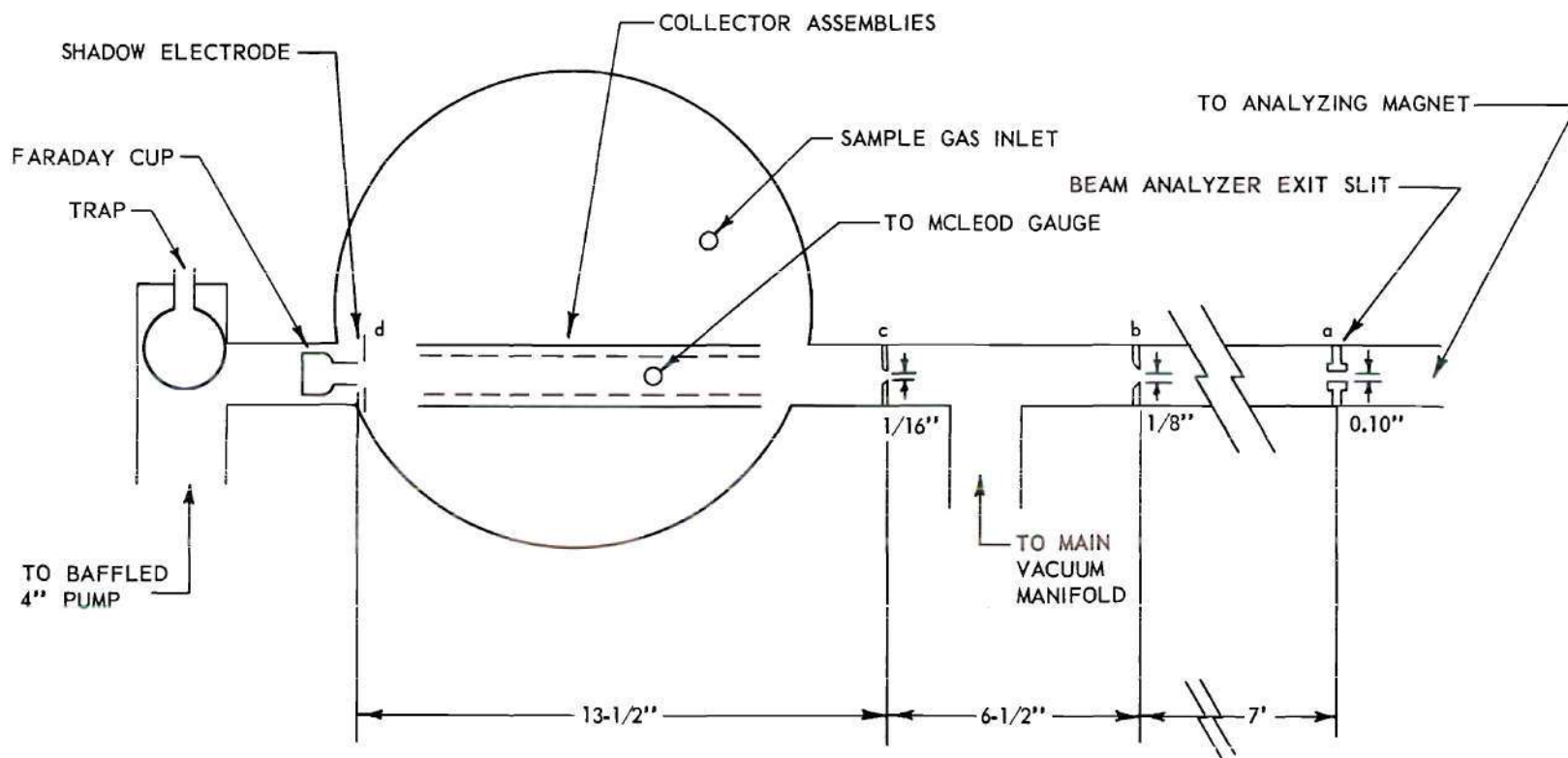


Figure 1. Schematic View of Apparatus for Gross Ionization Measurements.

through  $90^\circ$  in an analyzing magnet, which assured that it consisted essentially only of protons. The proton energy was stabilized by electronic regulation of the accelerator voltage to maintain equal currents on the two slit edges at "a," which amounted to demanding a constant deflection in the regulated magnetic field. (This was the standard stabilizing system provided by the accelerator manufacturer, the High Voltage Engineering Corporation. The nominal energy spread was  $\pm 2$  kev at 1 Mev.) Thus the particle energy was determined by the value of the magnetic field and was measured by measuring that field. Employed for this purpose was a Harvey Wells model G-501 nuclear magnetic resonance gaussmeter, which as used had relative and absolute accuracies of one part in  $10^3$ . The deflection geometry was calibrated empirically by measuring the magnetic field corresponding to the 1.019-Mev threshold of the nuclear reaction  $H^3(p,n)He^3$ , using a tritium-zirconium target.

Referring again to Figure 1, the round, knife-edged apertures "b" and "c" were machined through 1/2-inch thick brass plates which, except for the apertures, were vacuum-tight closures of the beam tube. With this arrangement, there was no noticeable rise of pressure in the accelerator vacuum system when the collision chamber was filled with hydrogen to its highest working pressure of  $10^{-3}$  mm Hg.

Collimation of the 1/16-inch diameter beam emerging from aperture "c" into the collision chamber was determined by that aperture and by the 0.10-inch analyzer exit slit at "a." (The beam width perpendicular to the page at "a," observed visually with a fluorescent "viewer" target, was also of the order of 0.10 inch.) The maximum angular divergence from the axis which an emerging particle could have was only about 4 minutes,

unless it had been scattered. The knife-edged design of apertures "b" and "c" minimized scattering from their edges, and the geometry permitted very few particles that had been scattered by residual gas in the beam tube to pass both "b" and "c". All components to the left from "b" were aligned with one another optically, and the entire assembly was oriented with respect to the analyzing magnet so as to maximize the current delivered to the Faraday cup at the left.

Because of the large distance between "a" and "b" (the analyzing magnet was in a different room from the rest of the apparatus), the beam impinging on aperture plate "b" remained diffuse even with optimum adjustment of the accelerator focus controls. As a result the beam emerging from "c", at 1.0 Mev, contained at best only about 0.8 microamperes of the 30 microamperes incident at "b". As the energy was reduced from 1.0 Mev, the beam became more diffuse and the transmitted intensity correspondingly lower. However, in all cases considered, the accompanying increase in the cross section compensated to the extent that uncertainties directly attributable to low intensity were not significant.

The Collision Chamber.--A photograph of the open collision chamber is shown in Figure 2. The collimated beam entered from the right and passed between the two identical electrode assemblies and into a Faraday cup located in the pump-out arm to the left. Electrical connections from the electrodes passed to the outside through 16 kovar-glass seals in the rear wall of the chamber. The chamber was evacuated by the four-inch baffled oil diffusion pump at the left. In the photograph, the cylinder at left above the pump initially contained a throttle valve arrangement



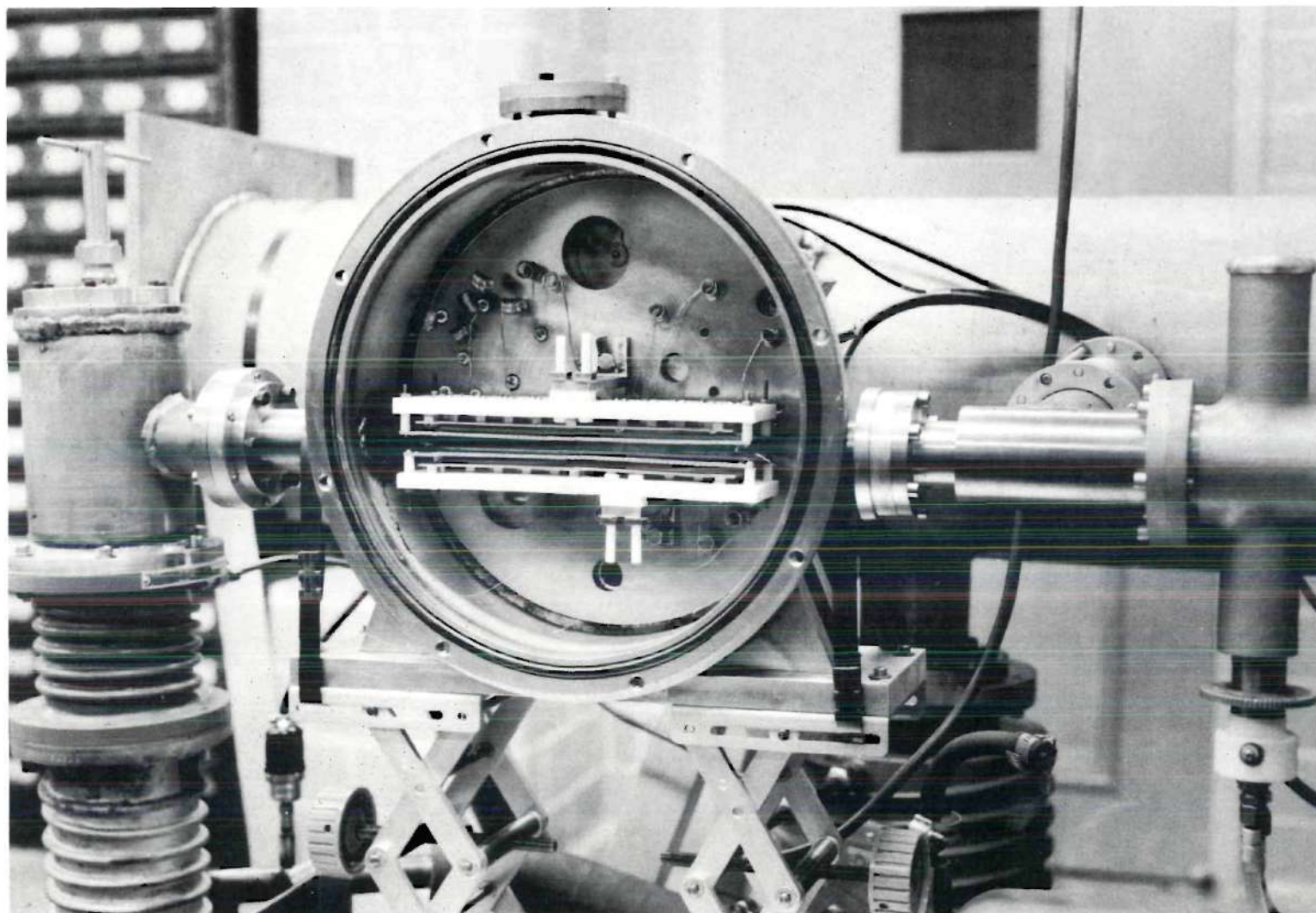


Figure 2. Interior View of the Collision Chamber.

actuated by the rod extending from the top of the assembly. This throttling valve was used during tests which were made to insure that no pressure gradients existed in the chamber at operating pressures. The valve was later replaced by the small pyrex flask shown in Figure 1, which served as a liquid nitrogen cold trap. Additional pumping was provided by a 2-inch connection from the large hole at the top of the back wall into the large vacuum manifold in the background. This connection was normally partially or completely closed off by a rotating valve arrangement (visible in the hole) which could be rotated to the open position by manipulation with an external hand magnet. Two ionization vacuum gauges were attached at holes visible in the lower part of the chamber, and a cold-trapped McLeod gauge was connected to a hole, hidden by the electrode assemblies, that looked directly into the space between the assemblies. The McLeod gauge was read with a cathetometer. Hydrogen gas was admitted through a palladium leak attached to one of the holes at the upper right. Other target gases were admitted through a mechanical leak after being passed through a cold trap.

The effective pumping aperture to the main pump on the left was deliberately severely constricted by the placement of the Faraday cup in the pump-out arm. The pump was operated continuously, even during a run when the target gas was in the chamber at the working pressure. The constriction was adjusted so that the resulting throughput of gas did not exceed the capabilities of the associated forepump. Working pressure was maintained by a continuous input of fresh target gas and was varied throughout the working range from  $10^{-4}$  to  $10^{-3}$  mm Hg simply by adjusting the input rate. The object of this constant pumping was to keep the

impurity level in the chamber essentially constant, independent of the working gas pressure. Thus, the ionization currents due to impurities arising from outgassing of interior surfaces and back-diffusion of pump oil vapor, which were measured with no target gas input, could be subtracted directly from all the readings with target gas present. In the course of all the measurements this "background gas" correction ordinarily amounted to only 2 to 5 per cent. The ultimate pressure in the chamber, obtained by closing the gas inlet, was too small to be read meaningfully with the McLeod gauge. It was measured by the ionization gauges to have an average value of almost  $6 \times 10^{-6}$  mm Hg, using the gauge manufacturer's nominal calibration for nitrogen. This was assumed to give only the general order of magnitude, however, since the composition of the background gas was unknown.

Detailed comparison of the readings of the two ion gauges with various gas throughput rates showed no significant pressure gradient between the two gauge locations for any gas input setting that provided an equilibrium pressure within the working range.

Measurement of the Incident Beam Intensity  $I_1$ .---The Faraday cup which collected the incident protons after they had traversed the collision volume was a bottle-shaped copper cup whose diameter was smallest at the open neck. The 1/2 inch inside diameter of the neck subtended an angle of  $2^\circ$  at the entrance aperture, "c", and about twice that angle at a point on the beam axis at the center of the effective collision volume. Both theoretical and experimental evidence indicated that fast incident protons would scatter more than  $1^\circ$  in far less than one per cent of all collisions.<sup>5</sup> With the "thin target" gas density used in these experiments,



fewer than 2 per cent of the incident protons underwent any sort of ion-producing collisions, and the number undergoing large angle elastic scattering collisions should have been negligible. It was expected that far less than one per cent of all incident particles would fail to enter the collection cup. To check this experimentally, a larger cup having a one-inch square opening was tried, and this gave values for the cross sections identical to those from the smaller round cup within all the other experimental uncertainties.

A disk-shaped "shadow" electrode with a sharp-edged circular aperture just smaller than the inside diameter of the mouth of the cup was located immediately in front of the cup and intercepted those few particles which had scattered through an angle so large that they would not have entered the cup. If not stopped, such particles might have struck the outside of the cup and released secondary electrons, resulting in a false increase in the apparent collected current. This "shadow" electrode was held at a negative potential with respect to the Faraday cup to suppress the escape of secondary electrons from the interior of the cup. In Figure 3 the collected current for constant incident beam intensity is plotted as a function of the suppression voltage. The lower curve applies to the bottle-shaped cup and shows that the apparent current was too high by over 10 per cent when there was no suppression, despite the deep design of the cup. The current assumed a constant asymptotic value for suppression voltages exceeding about 30 volts. The convenient value of  $67\frac{1}{2}$  volts was subsequently used throughout the measurements.

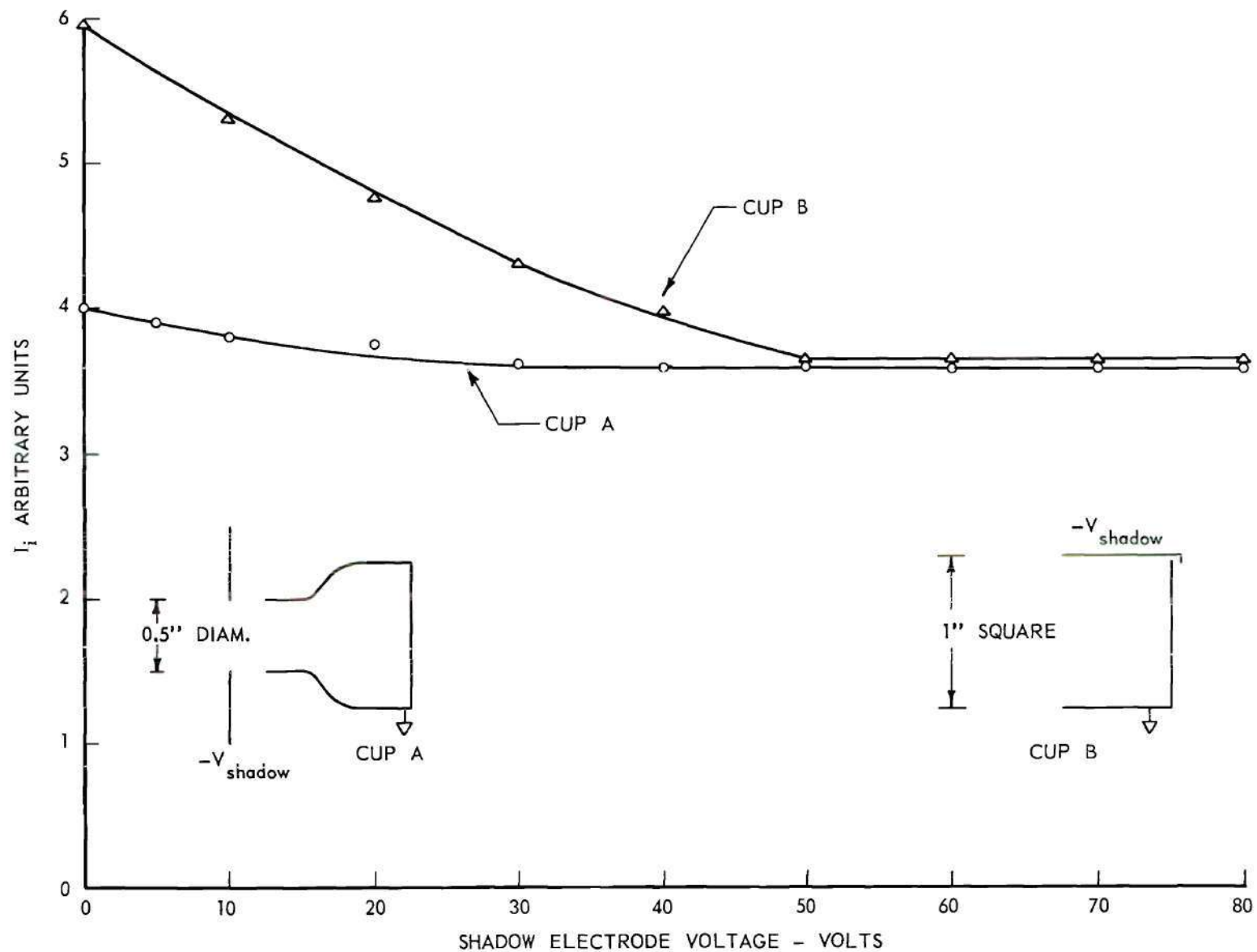


Figure 3. Incident Beam Collected in Faraday Cup Versus Suppression Voltage.



The upper curve in Figure 3 was obtained with the second Faraday cup mentioned previously, which was a box one-inch square and  $7/8$ -inch deep. There was no "shadow" electrode in this case, but one side wall of the box was held negative to provide suppression. As expected, with the more open design of this cup, a larger suppression voltage was required to reduce the current to its asymptotic value. The two curves are arbitrarily scaled to approach the same asymptotic value to reflect the fact, mentioned earlier, that using either cup in the cross section measurement gave the same result within all other experimental uncertainties. The bulk of the data presented in the results was obtained with the round cup.

The Collector Assemblies and Electrometers.--A photograph of one of the two identical slow-particle collector assemblies is shown in Figure 4. The collector plate had nine segments, each separately mounted to the rigid  $3/8$ -inch teflon backing, with its front surface  $1/4$ -inch in front of the backing. The five center segments were all cut to an accurate length of  $1.106 \pm .001$  inches in the beam direction, and all segments were accurately spaced  $0.010$  inches apart. All nine sections were always held at the same potential, so that the field in front of the assembly was essentially the same as if it had been one large continuous plate. However, only the ion (or electron) currents collected by one or more of the five central segments were ever included in the electrometer circuit for measurement. The remaining segments served as guards to assure that the field in front of the active segments was parallel and uniform, so there would be no edge effects due to fringe fields. Thus the "effective volume"

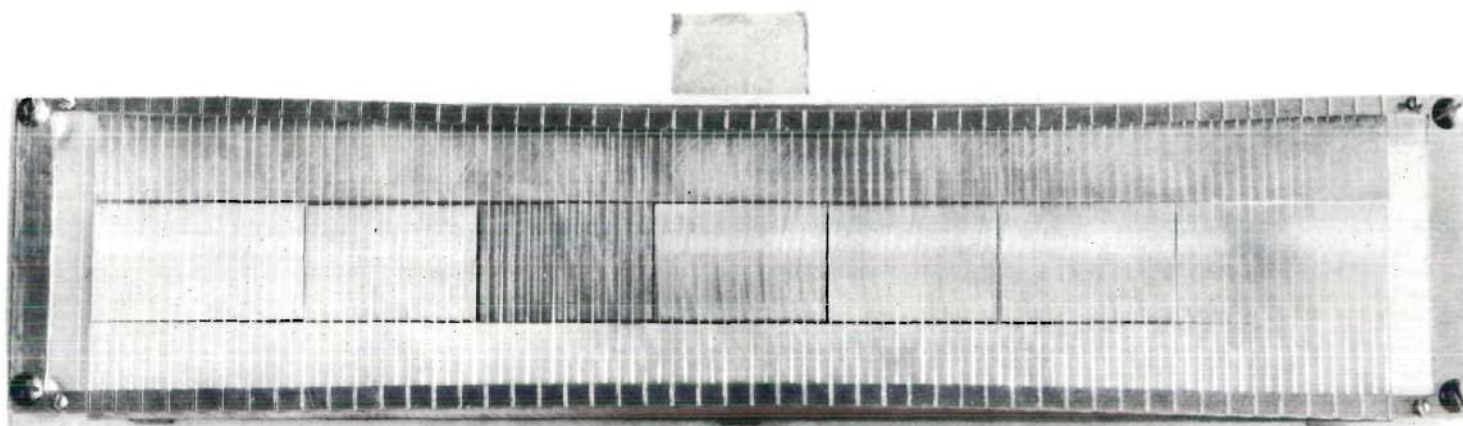


Figure 4. Single Electrode Structure.

of the target gas from which the ions were drawn was the rectangular parallelepiped defined by the active segments of the two collector assemblies. Edge effects at one end of this volume which were due to forward momentum of the slow ions should have been exactly compensated by the same effects at the other end, since the incident fast beam was not attenuated or scattered appreciably across the volume.

Each of the five central segments of each assembly had a separate lead to the outside, so that changes in the number of active segments could be made externally. The proportionality of the "effective volume" to the number of active segments was tested experimentally. The currents collected to one, to three, and to all five segments, corrected for leakage and normalized to the same incident beam intensity, were found to lie in the ratio of 1:3:5 within all other experimental uncertainties. Therefore, the target thickness used in computation of the cross sections was simply the combined length of all the active segments. In the bulk of the measurements only the three center segments were used, for which the target thickness was 3.318 inches.

Each collector assembly also had a grid, which can be seen in Figure 4. It consisted of 0.004-inch diameter stainless steel wires strung 0.100 inch apart on a brass frame, and was positioned  $1/4$  inch in front of the collector plate surface. Each grid was held negative with respect to its collector to suppress the emission of secondary electrons. While the plate which was held positive to collect electrons and negative ions would not really appear to need a suppressor, it was intended to make both collector assemblies as nearly identical as possible in order to achieve a high degree of symmetry. It was verified that there was no

change in the measured cross section values when the roles of the two collector assemblies were interchanged. The ion transmission of these grids was assumed to be essentially equal to their geometric transmission, which was 96 per cent.

A significant fraction of the "slow" ions produced by energetic protons might in fact have had substantial energies of 100 ev and more, and their initial motion might of course be directed toward the wrong collector plate. A substantial "collection" field across the collision volume was required to assure that essentially all particles would reach the proper collector. Actually, the collection field was determined by the potentials of the two suppressor grids. For symmetry, the two grids were maintained at potentials of equal magnitude but opposite sign with respect to the grounded chamber. This magnitude will hereafter be designated as  $V_c$  (c for "collection"). Each collector plate was positive with respect to its grid by an amount designated as  $V_s$  (s for "suppression"). Thus the electron collector was at the positive potential ( $V_c + V_s$ ), while the positive-ion collector was at the negative potential  $-(V_c - V_s)$ .

The magnitudes of  $V_c$  and  $V_s$  had to be chosen large enough that the collected currents would show saturation in that they would not change for any further increase of either  $V_c$  or  $V_s$ . The collected positive-ion current is designated  $I^+$ , the collected electron current  $I^-$ , and the incident beam current collected at the Faraday cup  $I_i$ . The observed ratios  $I^+/I_i$  and  $I^-/I_i$  for constant  $V_c = 750$  volts are plotted against  $V_s$  in Figure 5, for two different incident beam energies. Saturation was evidently achieved by  $V_s$  greater than 50 volts. The values  $V_s = 150$  and  $V_s = 100$  volts proved to be convenient and were used in the bulk of the measurements.



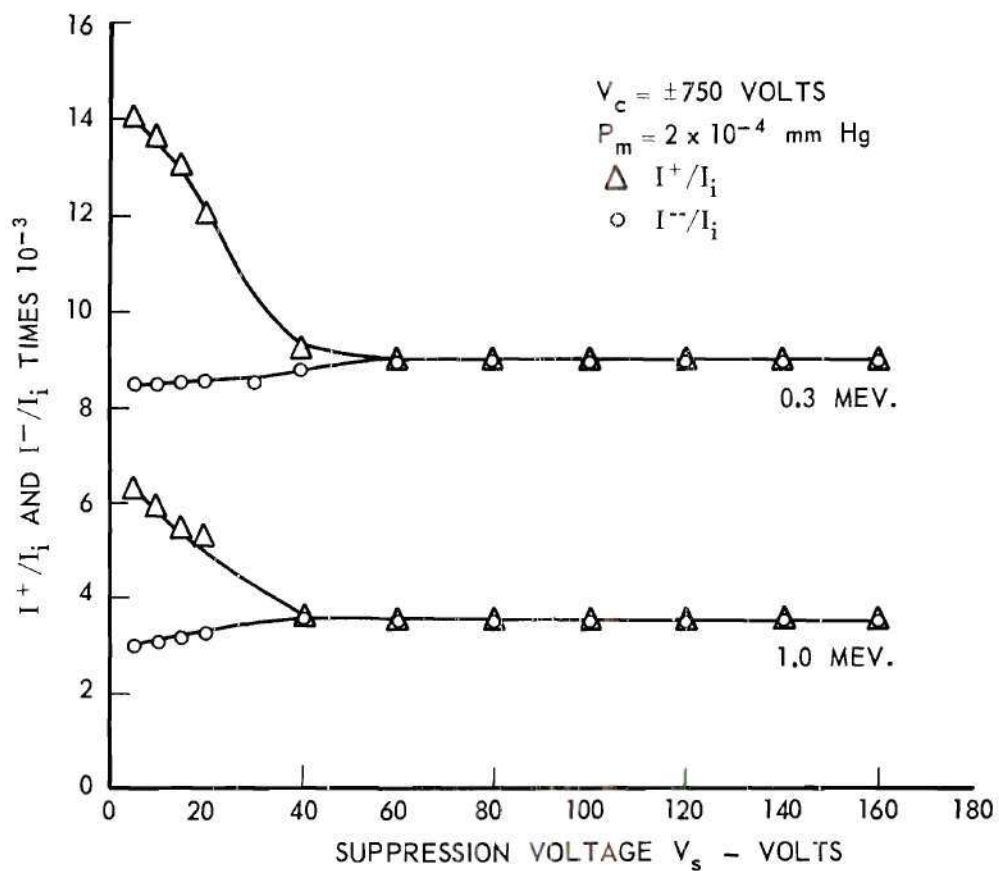


Figure 5. Apparent Ion Currents Versus Suppressor Grid Voltage for Constant Collection Field.



It will be noted in Figure 5 that the ordinate is not in arbitrary units. The saturation values of  $I^+$  and  $I^-$  were equal for all data runs, within the ability to read the meters, at both energies shown for protons incident on the target gases investigated. An anomalous case with higher electron than positive ion current arose following discharges in helium. The excess electron current apparently arose from the release of electrons from the grids by photon emission arising from the bombardment of the Faraday cup by the incident beam. This apparent grid surface sensitivity disappeared with time. A further discussion of this topic appears in Chapter VI. The current equality existing during data runs indicated that charge-transfer reactions were not making any appreciable contribution to the observed positive-ion current. Further, the small values of the ratio  $I^+/I_i$  (less than  $10^{-2}$ ) verified the earlier assertion that the target was "thin."

In Figure 6 are plotted the values of the gross ionization cross section  $\sigma_i$  at 1.0 Mev computed from measurements made with various values of  $V_c$  and constant  $V_s = 150$  volts. The scatter of the points reflects all of the several uncertainties which entered into this computation, and does not exceed the overall uncertainty to be discussed subsequently. It was concluded that saturation had already been reached at  $V_c = 450$  volts, the smallest value investigated. The values  $V_c = 900$  and 1050 volts were used in obtaining the bulk of the data for protons on argon, hydrogen, nitrogen, and carbon monoxide. The lower value  $V_c = 600$  volts was used for protons on helium, neon, and oxygen to alleviate a discharge condition which occurred in these gases. In some cases below 0.3 Mev incident proton energy, the collection voltage had to be removed while reading the

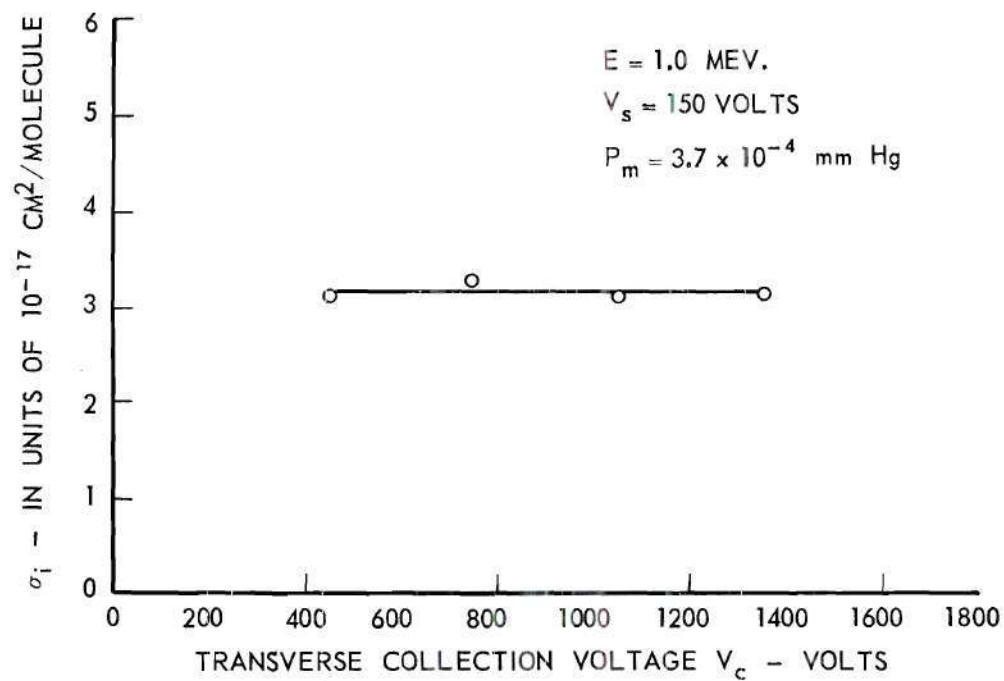


Figure 6. Observed Ionization Cross Section for Various Collection Field Strengths.

incident beam current, because it was found to deflect the incident beam off the opening of the Faraday cup. Complete runs at lower  $V_c$  of 750 and 450 volts, where this procedure was not necessary, gave identical results. The overall collection efficiencies were taken to be equal to the geometric transmission factors of the grids, or 96 per cent.

The two Keithley model 410 electrometers used for current measurements had to be floated from laboratory ground at the potentials of the collectors. They were isolated from their mounting rack by lucite blocks and were completely enclosed by a well-grounded screen cage. AC power was supplied through isolation transformers. The DC polarizing potentials were supplied by shielded battery packs which were also enclosed in the cage, because any ripple or noise in this supply was capacitively coupled into the electrometer input. Under these conditions, the noise in the electrometers with no input current was such as would have interfered with current measurements in the  $10^{-13}$  ampere range, but it was negligible for the smallest currents ( $2 \times 10^{-12}$  amperes) encountered in the measurements described.

The most serious source of noise in these experiments came directly from the behavior of the incident proton beam. Although the current entering the collision chamber had satisfactory long-term stability, its instantaneous value varied rapidly and erratically. Damping time constants provided by high quality shunting capacitors in the electrometer input circuits were added to reduce the meter jitter. In practice, one electrometer was used to measure either  $I^+$  or  $I^-$ , while the second was used for simultaneous reading of the incident beam intensity  $I_i$ . The two meters were in close physical proximity so that both could be seen at the

same time. The ratios  $I^+/I_1$  and  $I^-/I_1$  could be observed to an estimated 2 per cent maximum uncertainty, including both reading error and the inherent uncertainty of the electrometers.

A most important factor that has not yet been mentioned is that of leakage currents. The construction of the collector assemblies was such that the leakage paths from the active collector segments across the teflon mounting plate to the grounded collision chamber were long and of very high resistance, and the resulting leakage currents across the teflon were negligible. The leads to the kovar-glass seals in the chamber wall were stiff copper wires that did not touch any surface. Each of the leads from the outside end of a seal to the electrometer cage was doubly shielded by the use of a coaxial cable with a heavy rubber outer jacket, slipped inside an extra braided wire sleeve. Only the outermost shields were grounded, while the inner shields of all cables were held at the same potentials as their central current leads. The kovar-glass seals themselves were, however, unguarded since they were not of a doubly concentric type that would permit the same arrangement as in the cables.

A typical set of leakage currents to the positive-ion collector is shown in Figure 7 for several values of  $V_c$ , with  $V_s = 150$  volts. While not strictly ohmic, the currents were small and steady, and varied with voltage in a regular way. They reproduced well over periods of hours, although there was some day-to-day variation that was presumably related to atmospheric conditions. The leakage current was read at frequent intervals during all data runs. In the case of hydrogen it constituted a correction of less than 5 per cent to the ion current reading, and contributed a negligible uncertainty. Following the occurrence of



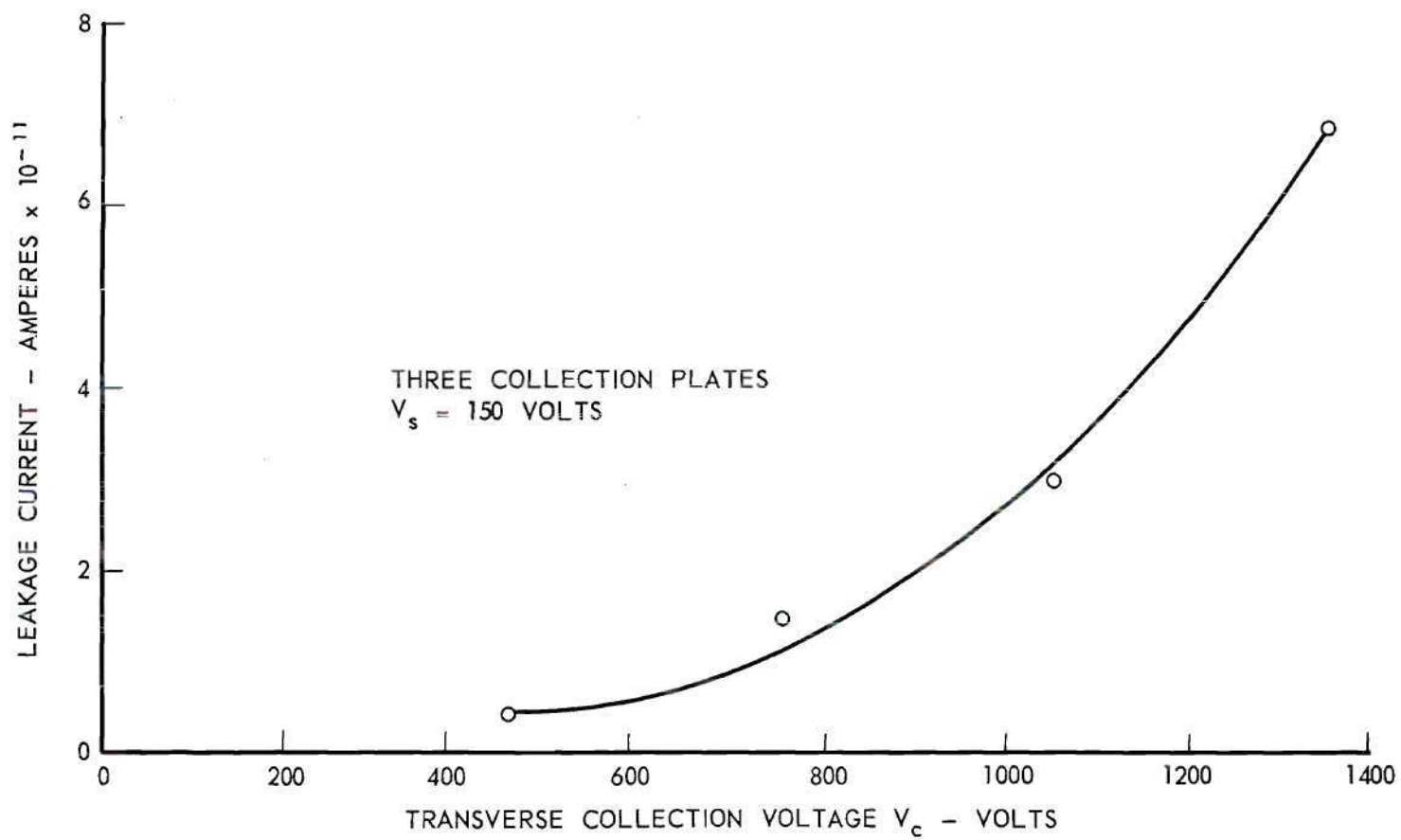


Figure 7. Leakage Currents Versus Collection Voltage.

discharges in helium, the internal leads in the chamber were consolidated with the result that leakage current corrections were negligible for all later runs. In all of the previous discussion all ion current readings mentioned had been corrected for leakage.

The arrangement of the high-voltage connections may be summarized as follows:

Each of the five central segments of a collector assembly had separate leads. A sixth lead was connected to all four of the outer guard segments, and a seventh to the grid. All seven leads passed out of the vacuum through separate kovar-glass seals, and through separate doubly shielded cables to a teflon patch board inside the electrometer cage.

The high-voltage tap of the polarizing battery pack was connected directly to the electrometer frame and to the inner shields of all seven cables. The physical arrangement was such as to avoid any "loops" for pickup.

The leads from the outer guard segments and from any "inactive" inner segments were also connected directly to the battery at the patch board.

The leads from all active segments were joined at the patch board and connected only to the electrometer input. The internal feedback arrangement of the electrometer limited the potential difference between the input and the frame to a few millivolts for any value of the input current, so that the active segments had essentially the same potential as the guards.

## CHAPTER IV

## EXPERIMENTAL RESULTS

Summary of Experimental Method.---The gross ionization cross sections for protons incident on helium, neon, argon, hydrogen, nitrogen, oxygen, and carbon monoxide were measured for incident particle energies over the range from 0.15 to 1.10 Mev. The incident proton energy was determined by  $90^\circ$  deflection in a regulated magnetic field, whose value was measured with a precision gaussmeter. The ionization currents of both signs were measured simultaneously with the incident beam current by means of sensitive electrometers. The target gas pressure was measured by a liquid-nitrogen-trapped McLeod gauge and ranged from 1.0 to  $12.0 \times 10^{-4}$  mm Hg. The effective collision volume was determined by the use of guard structures around the collector electrodes. Collection potentials of plus and minus 1050 and 600 volts were used for the bulk of the measurements. Suppression potentials of 100 and 150 volts were used on the collectors.

Data Corrections.---Leakage currents in the electrometer circuits were measured frequently and subtracted from all current measurements for which they had a significant value. The correction was usually less than 5 per cent. The constant pumping arrangement described in Chapter III was used to provide a residual background gas density that was independent of the sample gas density insofar as possible. In the case of hydrogen the target gas was admitted through a palladium leak which automatically

assured high purity of the entering gas. Other gases were admitted through a mechanical leak subsequent to liquid nitrogen or dry ice and acetone trapping.

The pressure of the residual gas averaged about  $6 \times 10^{-6}$  mm Hg as indicated by ionization gauges, using the nitrogen calibration. The actual value was uncertain since the composition was unknown. A typical run of the ionization currents produced in the residual gas is shown in Figure 8. The slope of the line is almost the same as that obtained with target gas in the chamber, and was not found to vary significantly from day to day. The impurity currents at several energies were read daily before the target gas was admitted, and again in most instances at the end of a day's run. The impurity ionization current for each energy inferred from these data was subtracted directly from each target gas ionization reading. Except for the lowest gas pressures, this amounted to a correction of less than 5 per cent.

In a given run the incident particle energy was varied over the entire range while the target gas pressure was held nominally constant. For the case of hydrogen, the setting of the palladium leak heater power was left fixed for at least one hour before readings were begun, to allow pressure equilibrium to be attained. This long equilibration time was not required when the mechanical leak was used. In all cases the McLeod gauge was read frequently during the run.

Complete runs were made for target gas pressures throughout the range from 1.0 to  $12.0 \times 10^{-4}$  mm Hg. The residual gas pressure was not subtracted from the indicated total pressure since it was not really well known; however, if it was really of the order of  $6 \times 10^{-6}$  mm Hg as the



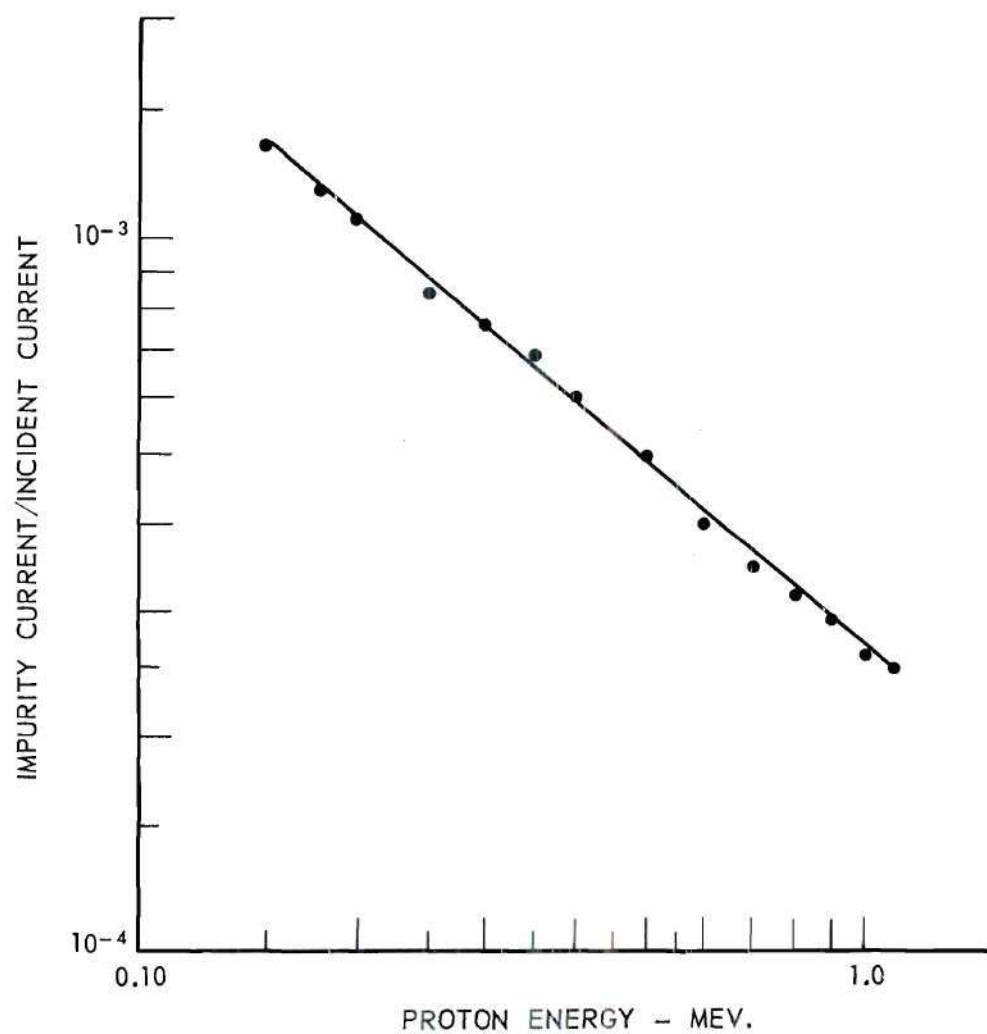


Figure 8. Impurity Contribution for Protons Incident on Background Gas.

ionization gauges indicated, it represented a correction of less than 5 per cent for all total gas pressures above  $1.2 \times 10^{-4}$  mm Hg. In computing the molecular density of the target gas, its temperature was taken to be that of the room.

A set of values obtained for the gross ionization cross section at one energy from a series of runs at different pressures of hydrogen gas is shown in Figure 9, plotted to a relative scale. The apparent fall-off at pressures below  $2.5 \times 10^{-4}$  mm Hg was identified with the above mentioned neglect of the contribution of the residual gas in computing the target gas density. Similarly, the indication of rising values for pressures above  $10 \times 10^{-4}$  mm Hg was identified with multiple collisions and failure of the "thin target" assumptions. The existence of a definite plateau between these regions lent confidence that all the important assumptions were valid there. All of the data used in compiling the final results were taken from runs lying within this plateau.

Results.--The final values for the absolute gross ionization cross sections for protons incident on helium, neon, argon, hydrogen, nitrogen, oxygen, and carbon monoxide are plotted in Figures 10 through 16. The data give an excellent fit to a straight line on a log-log plot throughout the energy range for all cases examined except carbon monoxide. The carbon monoxide data also fit a straight line for energies greater than approximately 0.400 Mev. The data therefore correspond, with the noted exception, to an expression of the form:

$$\sigma_i = A \times E^{-C} \text{ cm}^2/\text{molecule} \quad (16)$$

where E represents the incident particle energy.

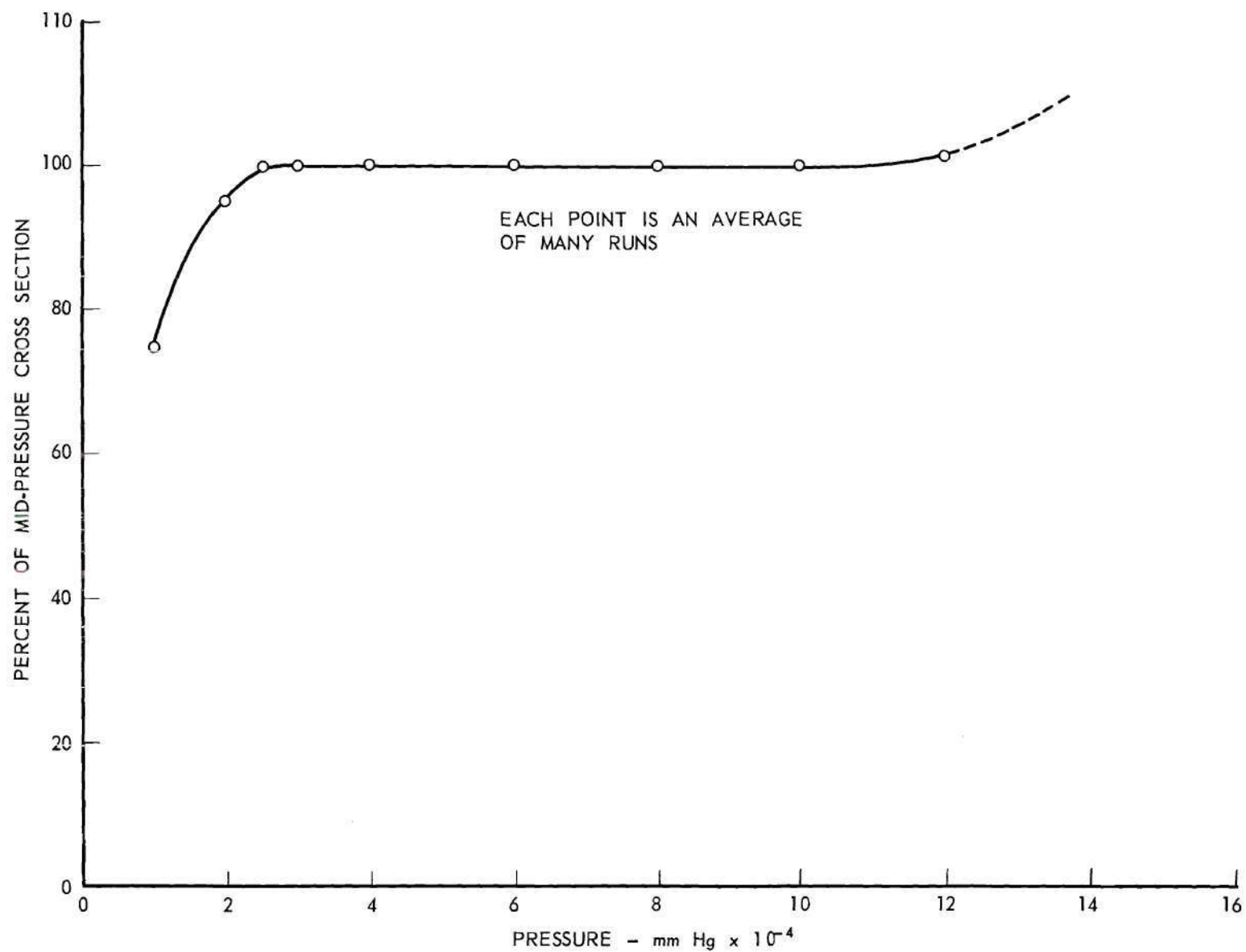


Figure 9. Computed Ionization Cross Section for Varying Target Gas Pressure.

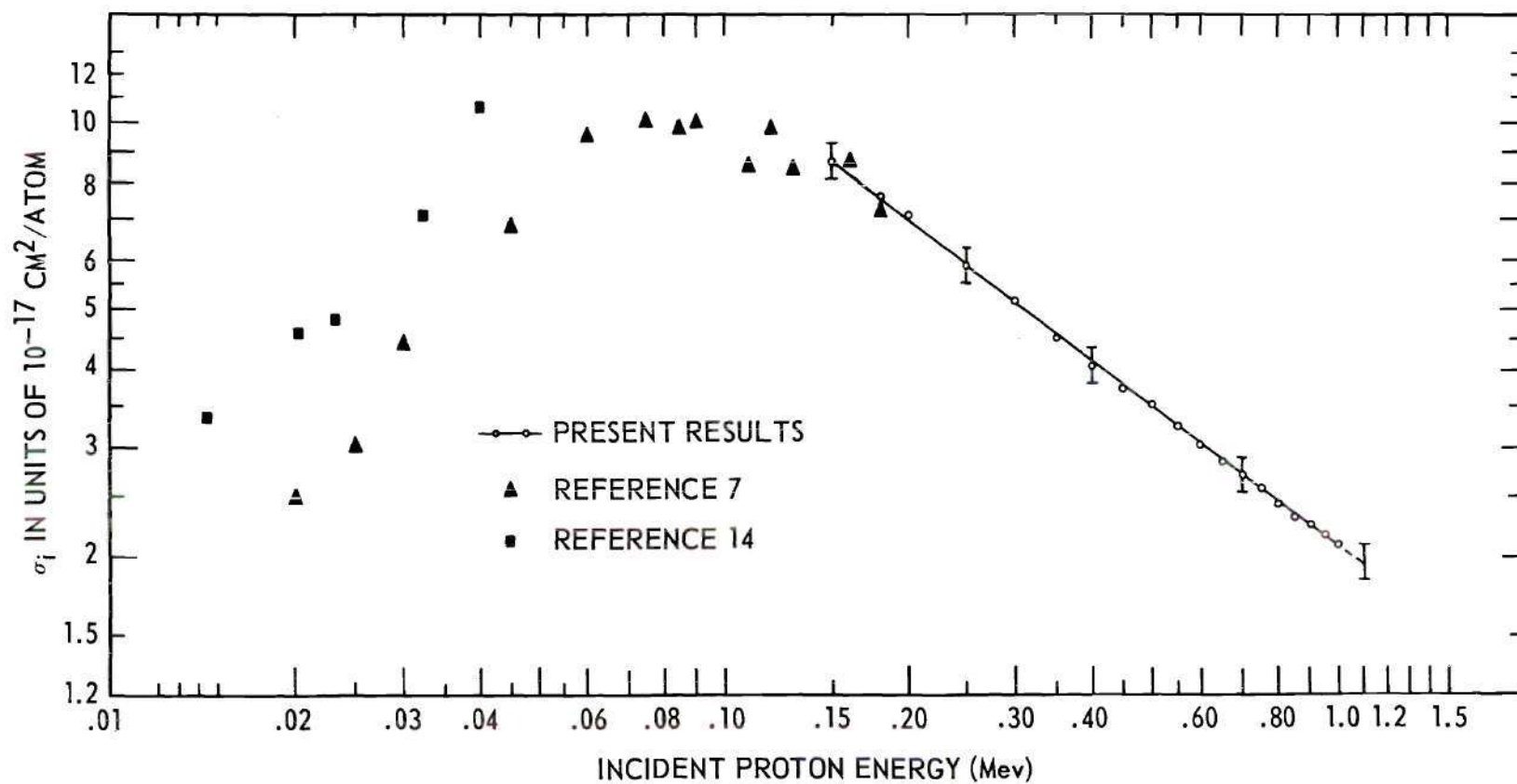


Figure 10. Gross Ionization Cross Section for Protons Incident on Helium.



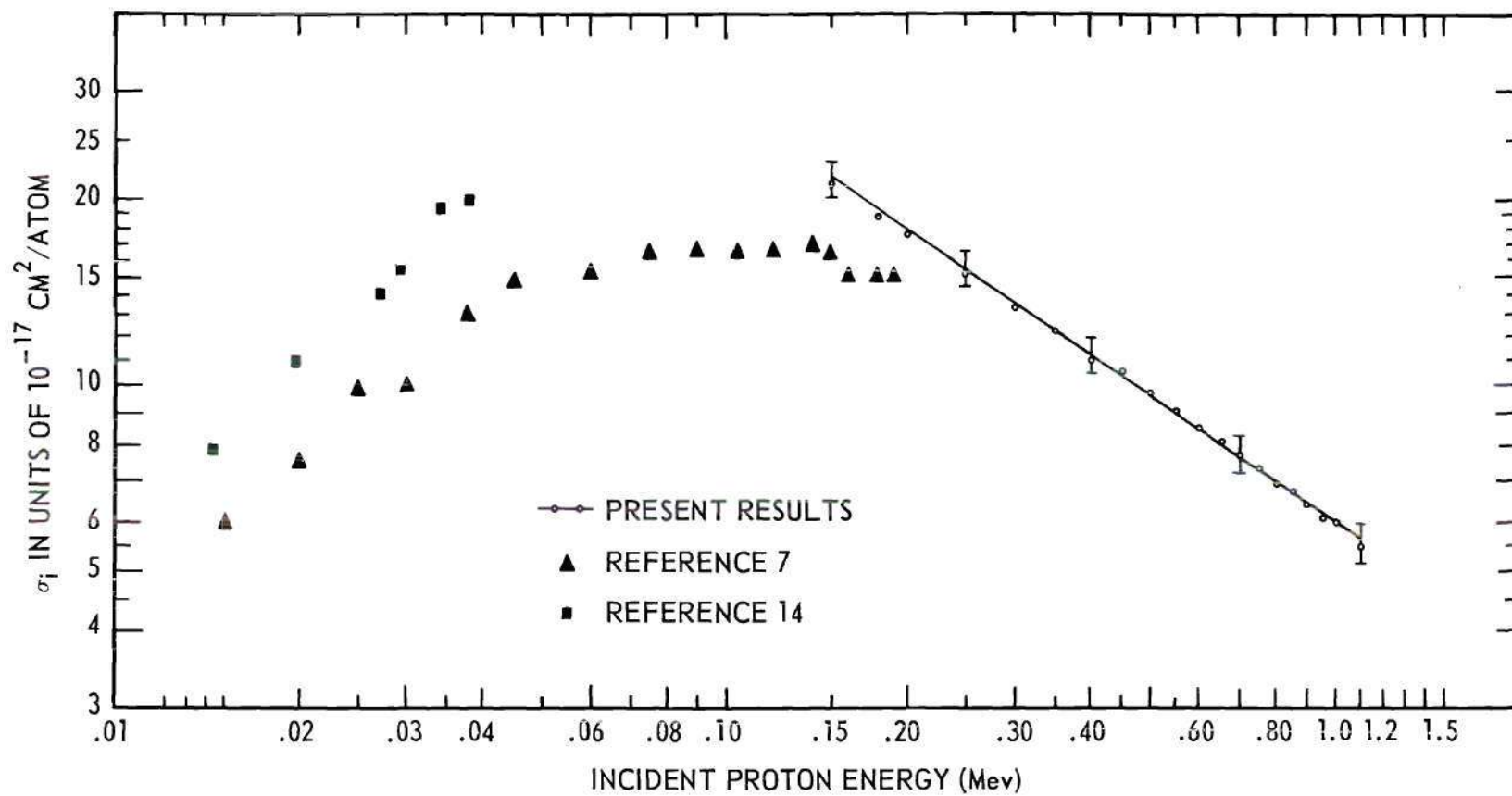


Figure 11. Gross Ionization Cross Section for Protons Incident on Neon.

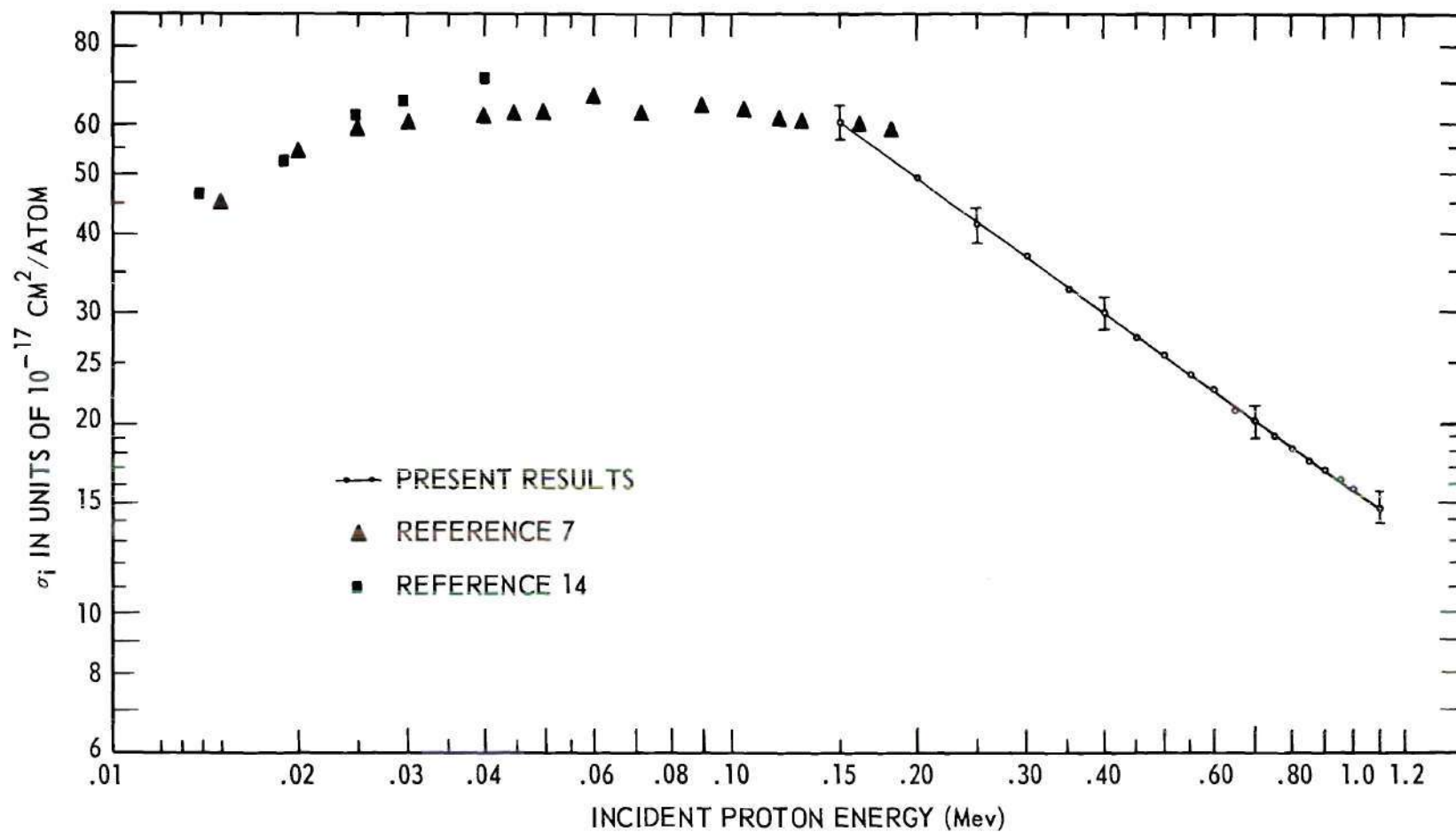


Figure 12. Gross Ionization Cross Section for Protons Incident on Argon.

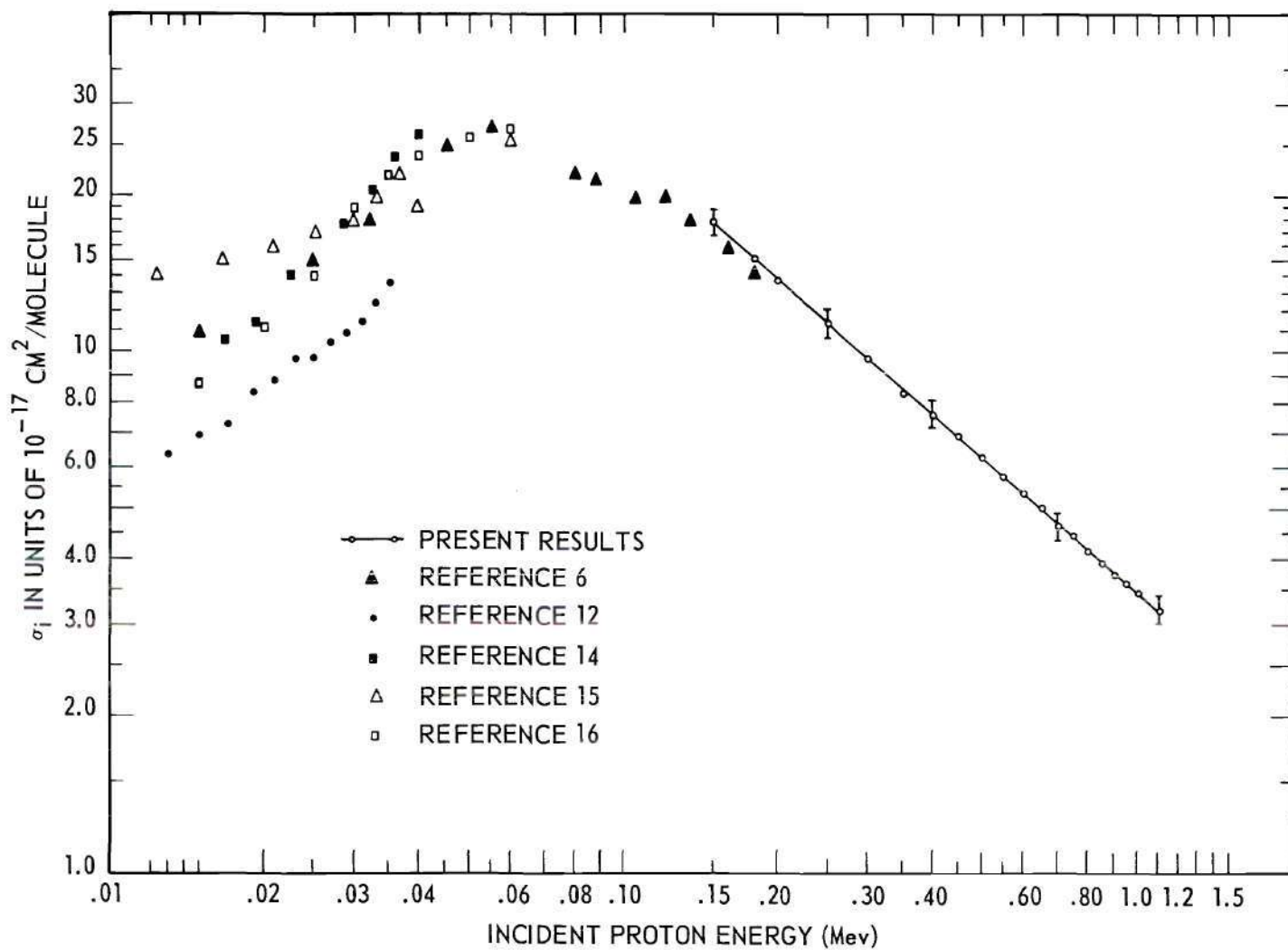


Figure 13. Gross Ionization Cross Section for Protons Incident on Molecular Hydrogen.

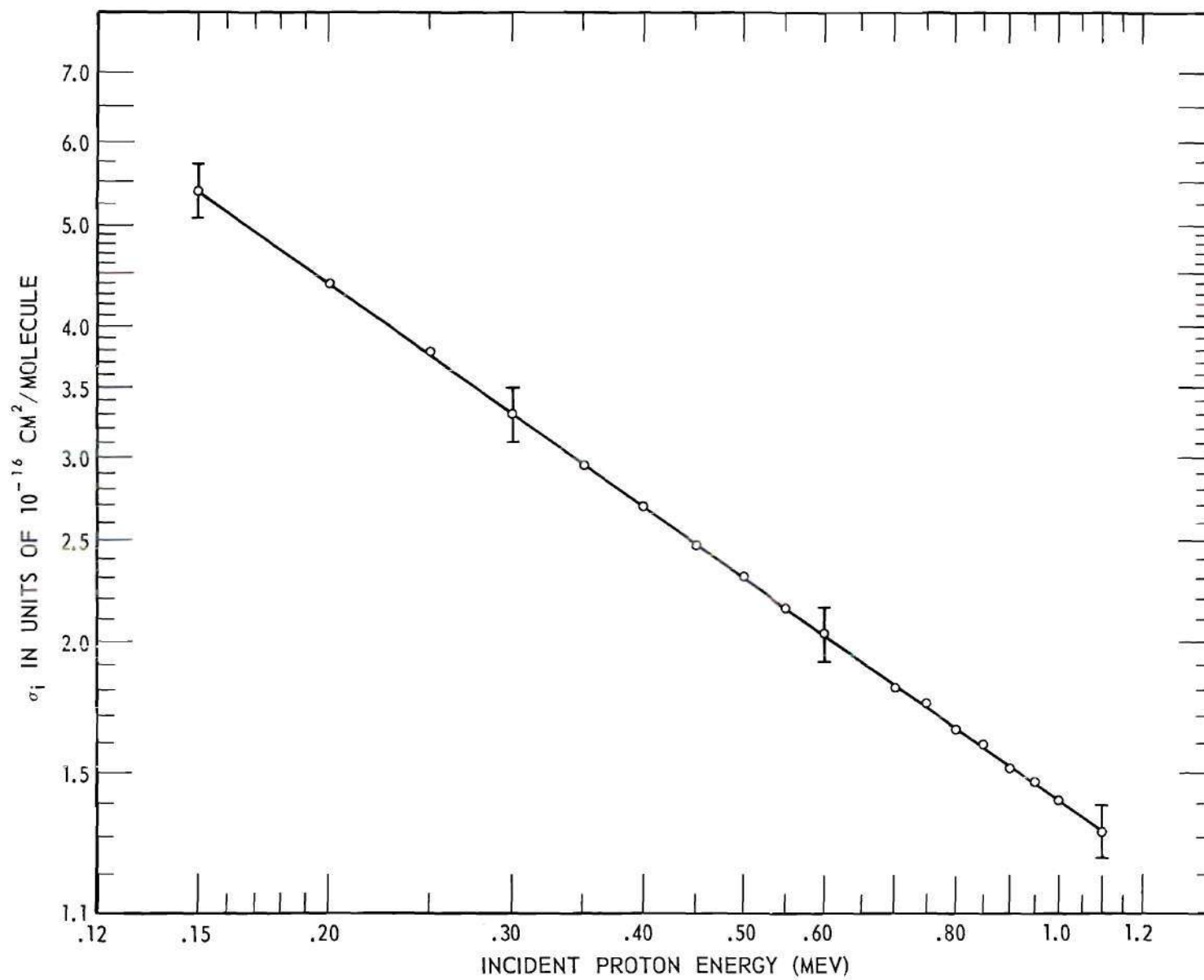


Figure 14. Gross Ionization Cross Section for Protons Incident on Molecular Nitrogen.



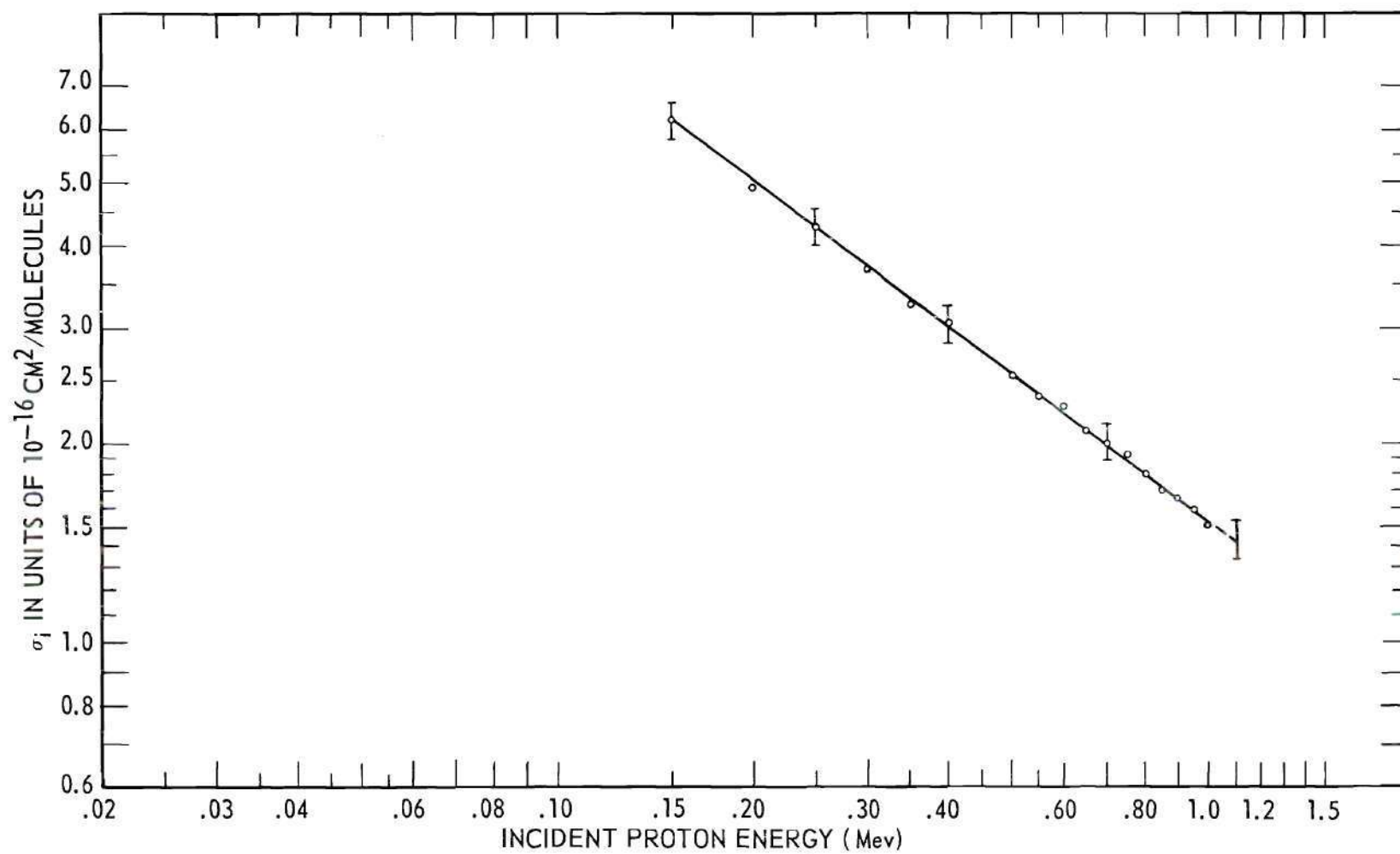


Figure 15. Gross Ionization Cross Section for Protons Incident on Molecular Oxygen.

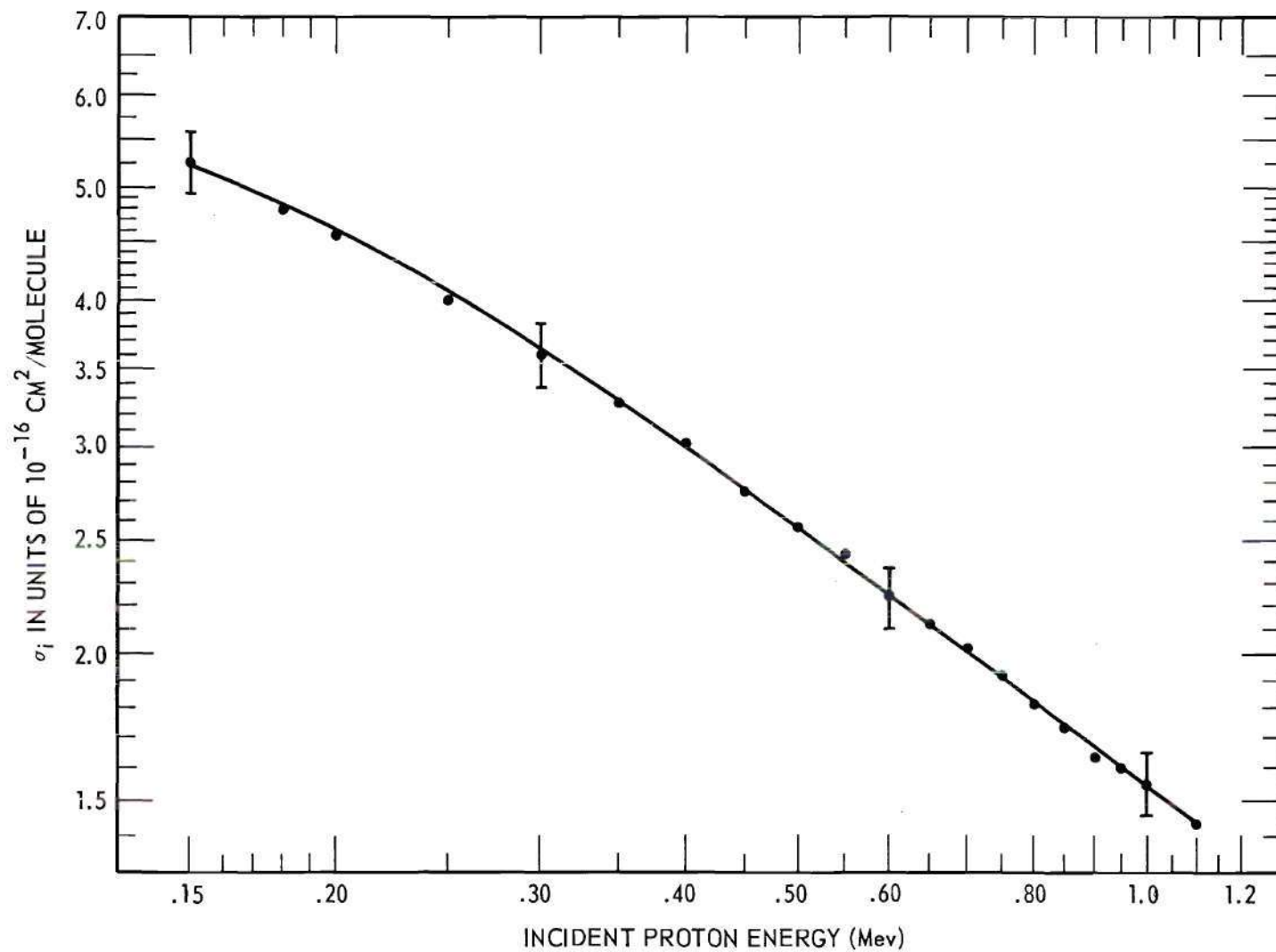


Figure 16. Gross Ionization Cross Section for Protons Incident on Carbon Monoxide.

An expression of this form has been fitted to the experimental data by a least squares method using a Burroughs 220 electronic computer. Values of the normalizing coefficient  $A$  and the exponent  $C$  obtained for the several gases studied are presented in Table 1 in the next section, together with the range of uncertainty of each that is indicated by the scatter of the data. The straight lines drawn in Figures 10-16 correspond to these computed values. Discussion of the possible error brackets shown on the curves is contained in the next section.

Discussion of Errors.--It was indicated in Chapter III that the uncertainty in a single reading of the ratio of the uncorrected ionization current to the incident beam current should not have exceeded about  $\pm 2$  per cent. The target gas temperature was not directly measured and may have been uncertain by perhaps  $\pm 1$  per cent. By far the largest uncertainty in these experiments lay in the measurement of the target gas pressure. Use of the cathetometer was believed to permit a relative reading accuracy of the McLeod gauge of less than 1 per cent in the range around  $5 \times 10^{-4}$  mm Hg. This gauge had not been absolutely calibrated, however, so that a possible error of about  $\pm 5$  per cent must be admitted in the absolute reading. This led to proportionate possible systematic error in the absolute magnitude of the cross sections, i.e., in the value of the normalization constant  $A$  in equation (16).

The slope of the curves is less uncertain than the cross section magnitudes. The proton energy had a nominal uncertainty of only  $\pm 0.2$  per cent at 1 Mev, and the uncertainty was believed to be not only  $\pm 0.5$  per cent at 0.15 Mev. Individual data runs were made at constant nominal

pressure, so the slopes obtained depended only on the relative scale-reading accuracy rather than on the absolute accuracy of the McLeod gauge. Any error in calibration of the energy due to uncertainty of the onset of the  $H^3(p,n)He^3$  reaction would likewise lead to a shifting of the curves without affecting their slopes.

A Burroughs 220 electronic computer was programmed to compute the values of A and C of equation (16) which corresponded to a least-squares fit to the average cross sections obtained from many individual runs, and to compute the probable errors in these constants that are indicated by the scatter of the data. The resulting values are given in Table 1 below.

Table 1. Calculated Values for the Equation  $\sigma_i = A \times E^{-C}$

Gas	$A \times 10^{-17} \text{ cm}^2/\text{molecule}$	C
He	$2.073 \pm 0.005$	$0.755 \pm 0.003$
Ne	$5.883 \pm 0.013$	$0.687 \pm 0.003$
Ar	$15.59 \pm 0.03$	$0.712 \pm 0.003$
H <sub>2</sub>	$3.433 \pm 0.009$	$0.864 \pm 0.004$
N <sub>2</sub>	$14.20 \pm 0.03$	$0.704 \pm 0.003$
O <sub>2</sub>	$15.26 \pm 0.11$	$0.747 \pm 0.007$
CO*	$15.47 \pm 0.05$	$0.733 \pm 0.009$

\* As explained in Chapter IV, the straight line relationship holds only above .400 Mev for this case.



The probable error of the normalization constant A that is computed from the scatter of the data can be seen to be less than 1 per cent in all cases. The previously mentioned possible error of about  $\pm 5$  per cent caused by uncertainty in the target gas pressure does not appear in these computed values since such an error is systematic. It is concluded that a possible error of  $\pm 6$  per cent must be admitted in the absolute normalization of the cross section curves and the flags shown on Figures 10-16 are of this magnitude.

It is emphasized that the relative values of the cross sections at various energies are not subject to this systematic error, and hence the uncertainties in the slopes of the lines are as indicated by the probable errors of the constant C in Table 1 above. Furthermore, the relative magnitudes of the cross sections for the various gases at a given energy are uncertain by no more than about  $\pm 2$  per cent.

The experimental results of other investigators<sup>6,7,12,14,15,16</sup> which are available in the lower energy ranges are included in Figures 10 through 16 for completeness. It is apparent that there is considerable disagreement in the low energy range among some of the results; however, the values of Afrosimov, et al.<sup>6</sup>, for protons in hydrogen, and Fedorenko, et al.<sup>7</sup>, for protons in neon and helium agree with the present results quite satisfactorily in the region between 0.15 and 0.18 Mev that overlaps the present results.

## CHAPTER V

## COMPARISON WITH AVAILABLE THEORY

Protons Incident on Molecular Hydrogen.--For the case of protons incident on molecular hydrogen, the gross ionization measurements yield in principle, as shown in Chapter II, the sum of the contributions from the following four distinct kinds of ionization events:



plus the three kinds of charge-transfer events:



Reactions (7) and (8) represent more complex events than do (5) and (6), and it seems quite likely that they are correspondingly improbable and contribute in a minor fashion to the total ionization. The sum of the cross sections for (2), (3), and (4) is the gross charge transfer cross section which has been measured previously<sup>4</sup>. This cross section is

found to be of such a magnitude that charge transfer should make a barely significant contribution of about 2 per cent at 0.15 Mev, but be negligible above 0.2 Mev. In verification of this assertion is the fact that the collected electron currents observed were always equal to the positive ion currents within the reading accuracy of  $\pm 2$  per cent. Any significant amount of charge transfer would have led to an excess of positive ion current over electron current. Any secondary electron emission produced by positive-ion impact on the grid shielding the slow-ion collector would have had the opposite effect. The data presented in Figure 5, Chapter III, indicate that this latter mechanism increased the electron current by less than 2 per cent. Therefore the gross ionization measurements yielded essentially the sum of the cross sections for processes (5) and (6).

Theoretical cross section calculations using the Born approximation have been made<sup>1</sup> for the atomic process:



A method of obtaining an approximate theoretical treatment for the molecular processes has been indicated in reference 1. Although the results calculated for reaction (16) were not given in explicit analytic form, the following generalization was made:

If a fast proton collides with a nucleus of atomic number  $Z_b$ , to which one electron is bound in the 1s state, then the cross section for removal of that electron takes the general form (Equation 21 of Reference 11):

$$\sigma^+ = \left(\frac{Z_b}{\Delta E}\right)^2 f\left(\frac{M\Delta E}{E}\right)$$

in which:

$\Delta E$  is the ionization energy for removal of the electron,

$M$  is the reduced mass of the colliding system,

$E$  is the kinetic energy of the relative motion,

$f$  is a function of unspecified analytic form.

This formula permits scaling of the graphical results given for reaction (17) to any other reaction that meets the above description.

It has often been assumed that a hydrogen molecule is simply equivalent in an energetic collision process to two independent hydrogen atoms, so that the molecular cross section would be expected to be simply twice the atomic cross section. However, in the formula above there is an explicit dependence on the ionization energy  $\Delta E$  of the electron to be removed. The vertical ionization energy of one electron in the hydrogen molecule is appreciably different from the atomic ionization energy, being, in fact, greater by the factor 1.2.

The scaling procedure followed was this: The molecule was considered to be equivalent to two free neutral atoms in every respect except that account was taken of the fact that the ionization energy is 1.2 times the normal atomic value. Ignored were the effects of the second atom on the reduced mass of the system consisting of the projectile and the first atom, on the ratio of the incident particle energy to the relative motion energy, and of course on the form of the electronic wave function that was used in the calculation of the atomic cross section. To this approximation, a theoretical cross section for the removal of one electron from the molecule by the impact of an incident proton of energy  $E$  will be twice the given atomic cross section for the



incident proton energy  $E/1.2$ , divided by  $(1.2)^2$ . This cross section should actually correspond to the sum of the cross sections for all of the several kinds of molecular ionization events, since the theoretical treatment made no restrictions on the final state of the molecule, and so the result should include all possible final states. Therefore, this cross section should correspond to the measured gross ionization cross section.

The dashed line in Figure 17 is the extrapolation from the theory of Bates and Griffing as described. Precision in plotting the line was limited by the accuracy with which the rather small graphs of the published paper could be read. There is essentially perfect agreement within the stated experimental uncertainties for high energies.

Protons Incident on Helium.--Theoretical calculations in the Born approximation of the cross sections for ionization and simultaneous ionization and excitation of helium by protons have been made by Mapleton.<sup>2</sup> He assumed that the helium wave functions may be approximated by products of normalized hydrogen wave functions in which the helium nucleus had an effective charge  $Z_1$  of 1.6875 for the ground state. He examined three cases corresponding to various choices for  $Z_2$  the effective charge associated with the Coulomb field acting on the final state bound electron, and  $Z_3$  the effective charge associated with the Coulomb field acting on the final state positive energy electron. These cases were:

$$\text{Case I:} \quad Z_2 = 2, \quad Z_3 = 1$$

$$\text{Case II:} \quad Z_2 = 2, \quad Z_3 = Z_1$$

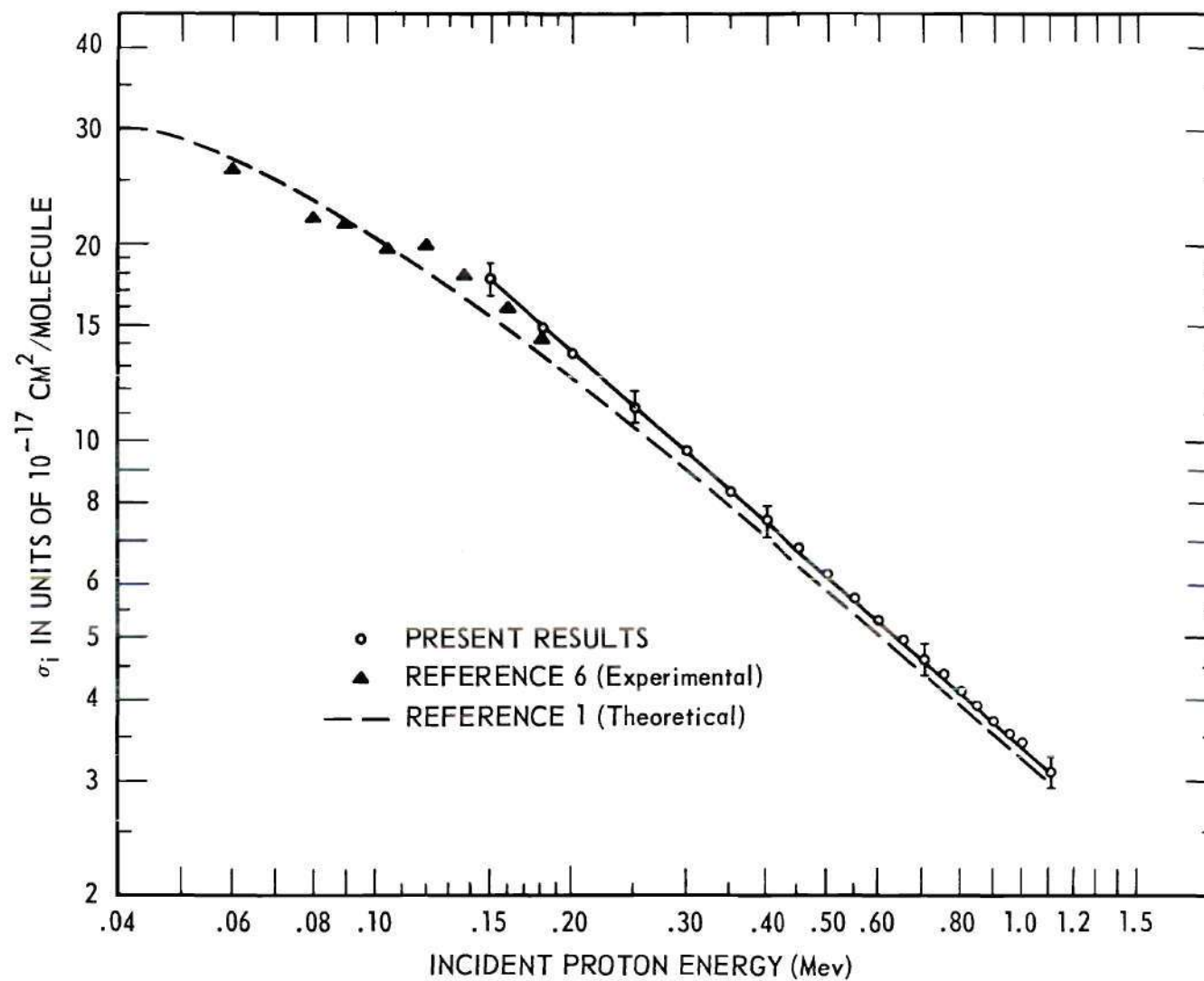


Figure 17. Comparison of the Experimental and Theoretical Gross Ionization Cross Sections for Protons Incident on Molecular Hydrogen.

Case III:  $Z_3 = Z_1$  for the  $\ell = 0$  term of the wave function  
of the final state positive energy electron

$Z_3 = 1$  for the  $\ell > 0$  terms of the wave functions  
of the final state positive energy electron.

Mapleton has pointed out that the cross sections determined from calculations based on the assumptions of Case III would be expected to be the most realistic. The dashed line in Figure 18 represents Mapleton's Case III result, plotted with rather poor precision because of difficulty in reading the small graphs of his published paper. There is essentially perfect agreement within the stated experimental uncertainties between the theoretical calculation and the experimental results in the energy range above approximately 400 kev.

Ionization cross sections for  $\alpha$ -particle impact and electron impact on helium have been calculated by Erskine<sup>17</sup> through an application of the Born approximation. Mapleton has demonstrated that it is possible to scale the  $\alpha$ -particle results to those for protons if particles with equal velocities of relative motion are considered. Translation of Erskine's results to the proton case leads to close agreement with Mapleton's Case III. It is also significant to note that Erskine's results for electron impact on helium are in close agreement with the experimental cross sections determined from the data of Smith.<sup>18</sup> This cross-correlation leads to added confidence in the experimental results for protons incident on helium obtained in this research.

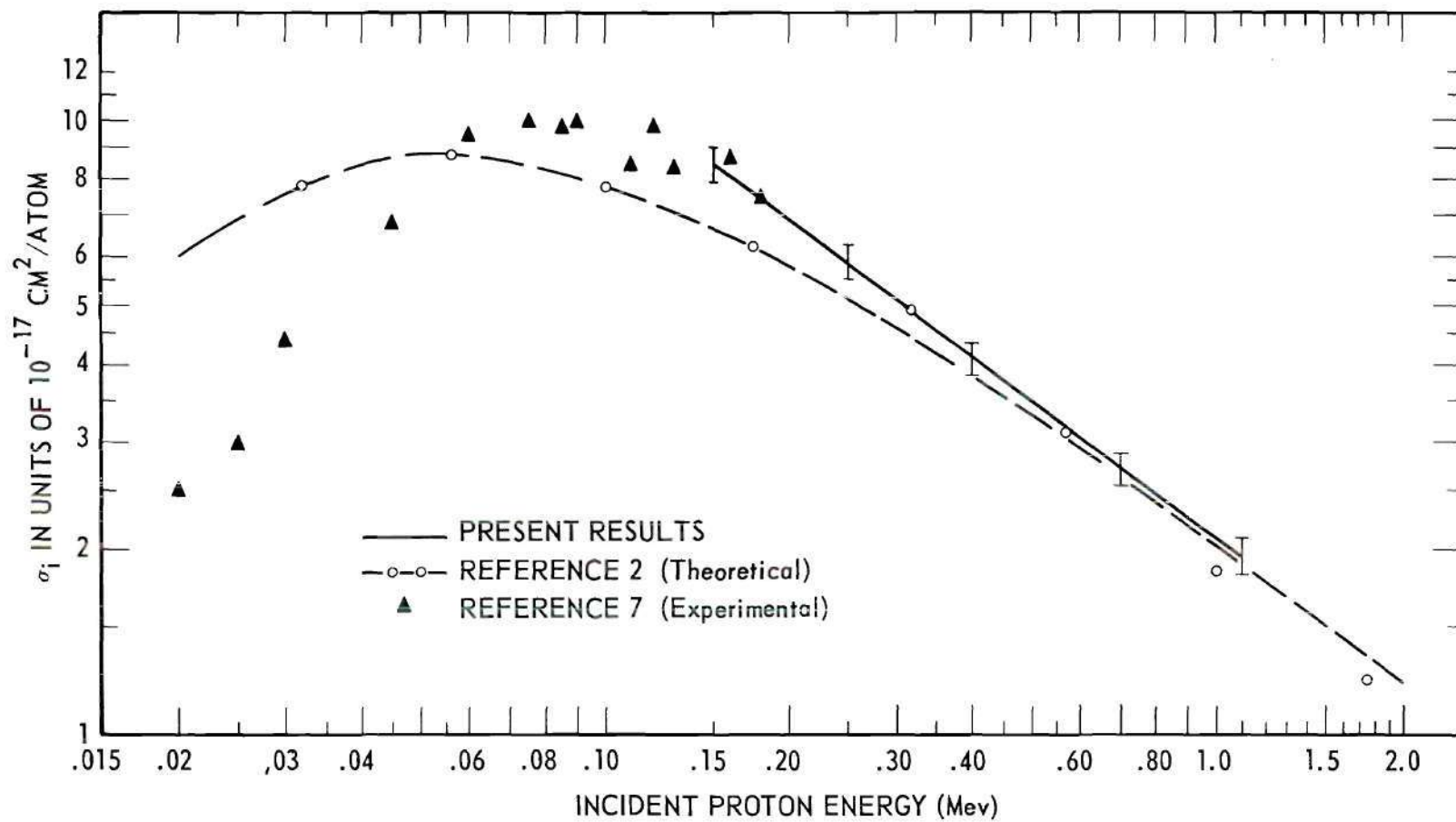


Figure 18. Comparison of Experimental and Theoretical Gross Ionization Cross Sections for Protons Incident on Helium.



Comparison of Experimental Cross Sections Obtained for Incident Protons

and Electrons of Equal Velocity.--It has been pointed out by Mott and Massey<sup>19</sup>, Bates and Griffing<sup>1</sup>, Mapleton<sup>2</sup>, and others that if the velocities of relative motion are the same, and are sufficiently high, the ionization cross sections for electron-atom and proton-atom collisions calculated in the Born approximation are the same. The velocity of relative motion is the same in both the laboratory and center-of-mass coordinate systems. It is possible to translate the electron cross section data by multiplying the electron energy scale by the ratio of the proton to the electron mass.

The known electron data corresponding to an energy range which is sufficiently high to be of interest in this comparison is limited in quantity and was obtained, for the most part, several decades ago. There appears to be reason to believe, however, that the bulk of the data is reliable. As an aid in evaluating the electron-molecule and proton-molecule comparisons some electron-molecule results in the energy range below the supposed lower limit of validity of the Born approximation are included. Data from the following sources appear, along with the proton-molecule cross sections obtained in this research, in Figures 19 through 25.

<u>Investigators</u>	<u>Gases</u>
Smith <sup>18</sup>	He, Ne, A
Tate and Smith <sup>20</sup>	N <sub>2</sub> , H <sub>2</sub> , O <sub>2</sub> , CO
Harrison <sup>21</sup>	H <sub>2</sub> , He
Tozer and Craggs <sup>22</sup>	A, Ne, He
Bleakney <sup>23,24</sup>	Ne, A, H <sub>2</sub>
Compton and Van Voorhis <sup>25</sup>	H <sub>2</sub> , He
Lampe, Franklin, and Field <sup>26</sup>	He, Ne, A, H <sub>2</sub> , N <sub>2</sub> , CO, O <sub>2</sub>

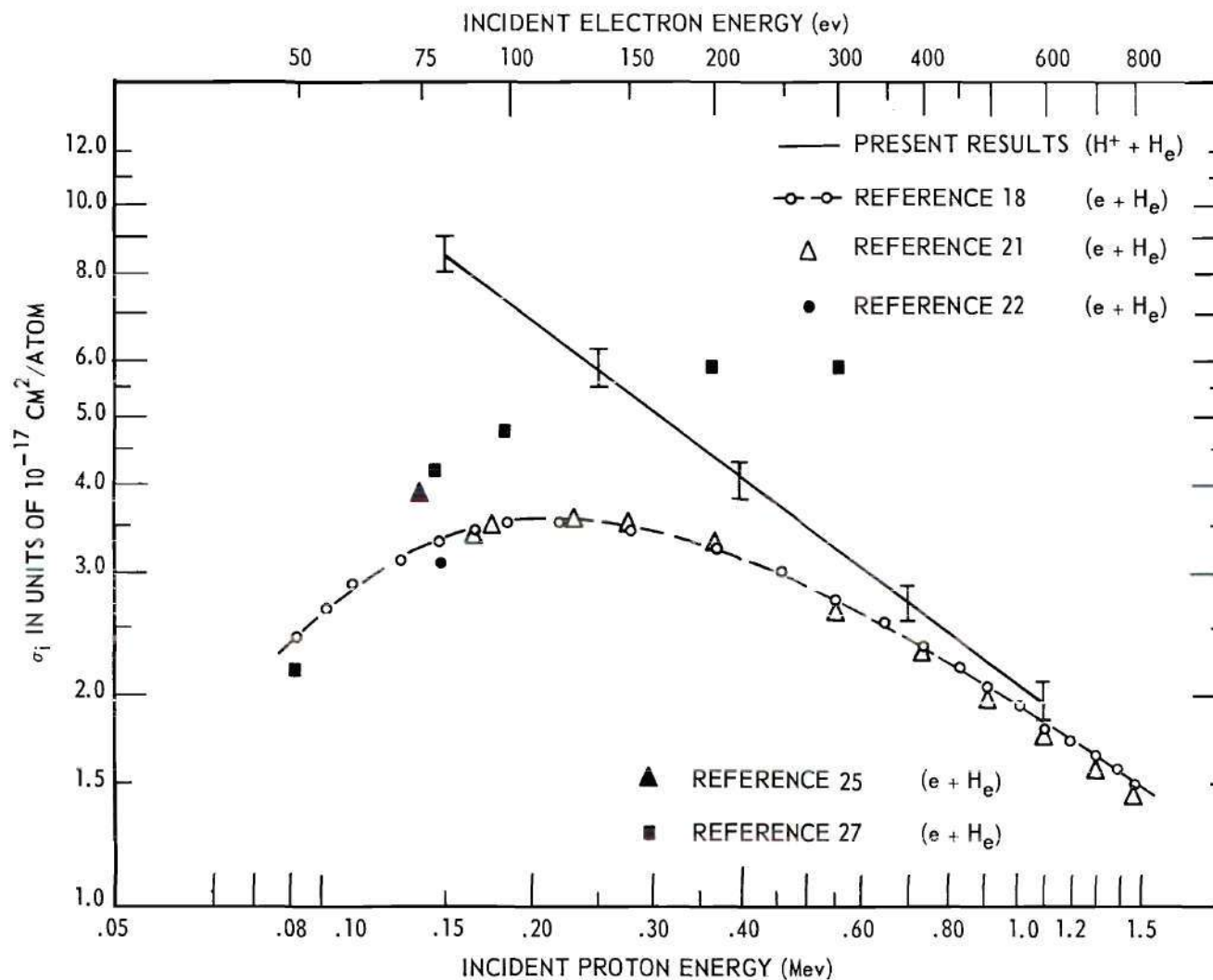


Figure 19. Comparison of Experimental Gross Ionization Cross Sections for Protons and Electrons of Equal Velocity Incident on Helium.

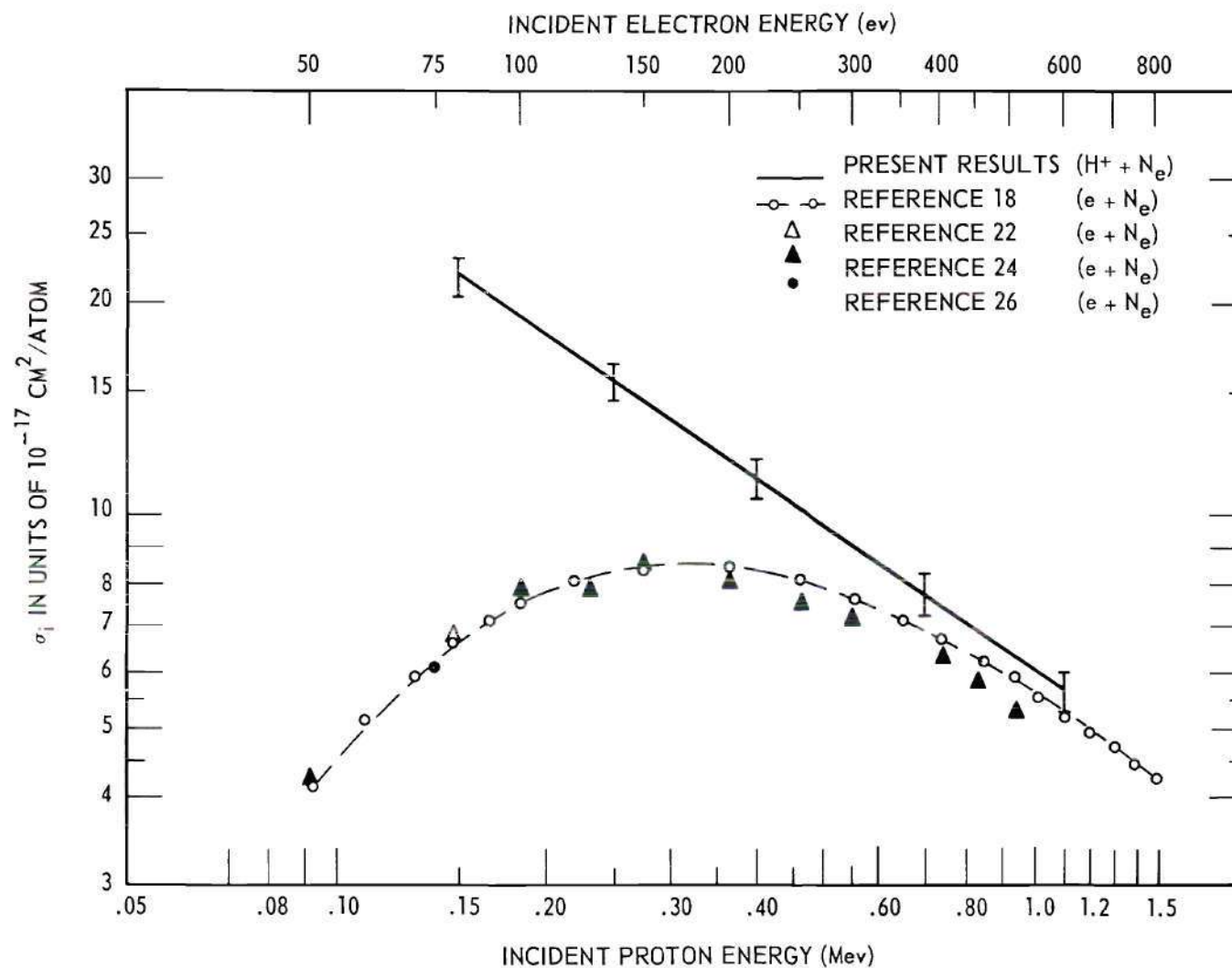


Figure 20. Comparison of Experimental Gross Ionization Cross Sections for Protons and Electrons of Equal Velocity Incident on Neon.

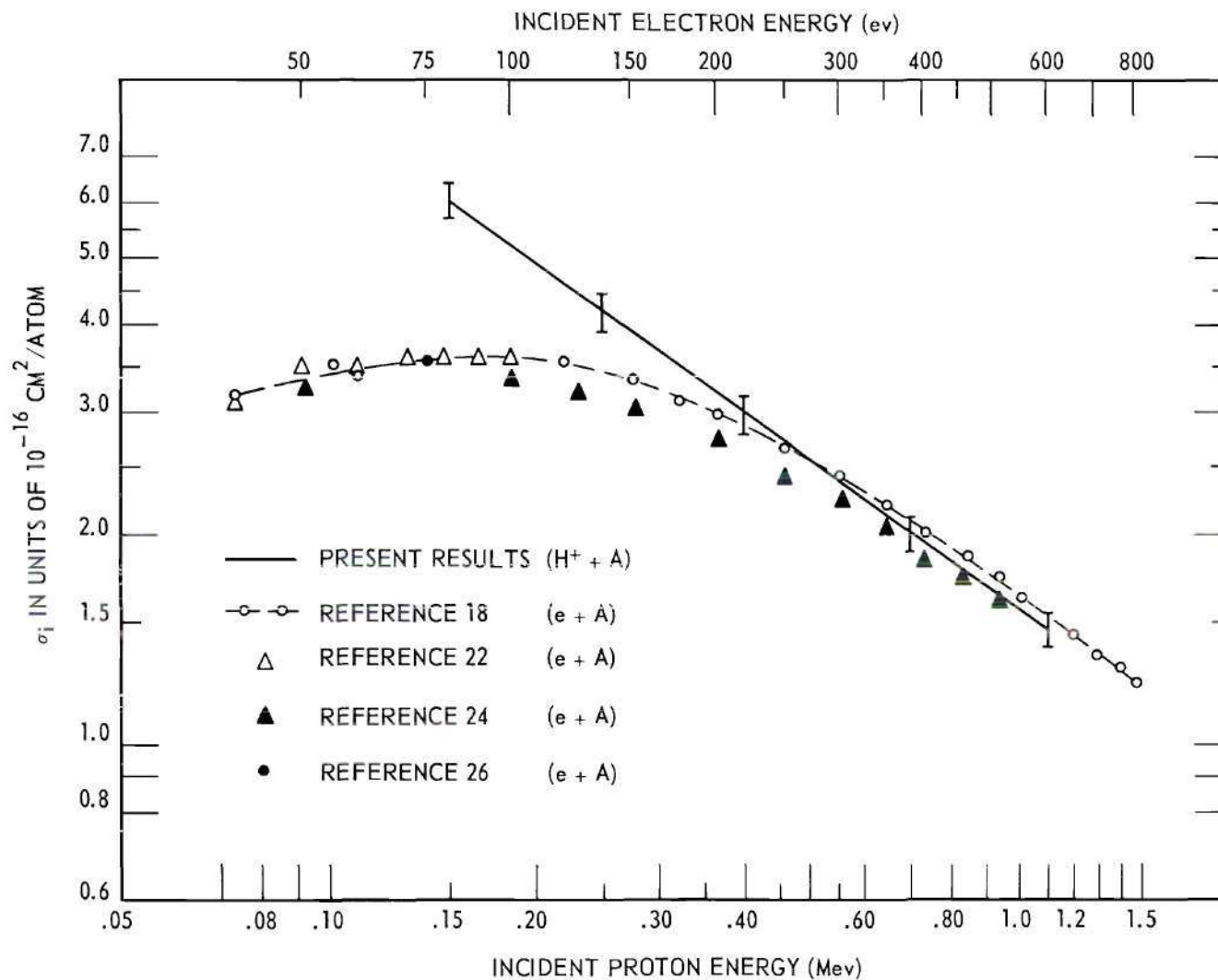


Figure 21. Comparison of Experimental Gross Ionization Cross Sections for Protons and Electrons of Equal Velocity Incident on Argon.

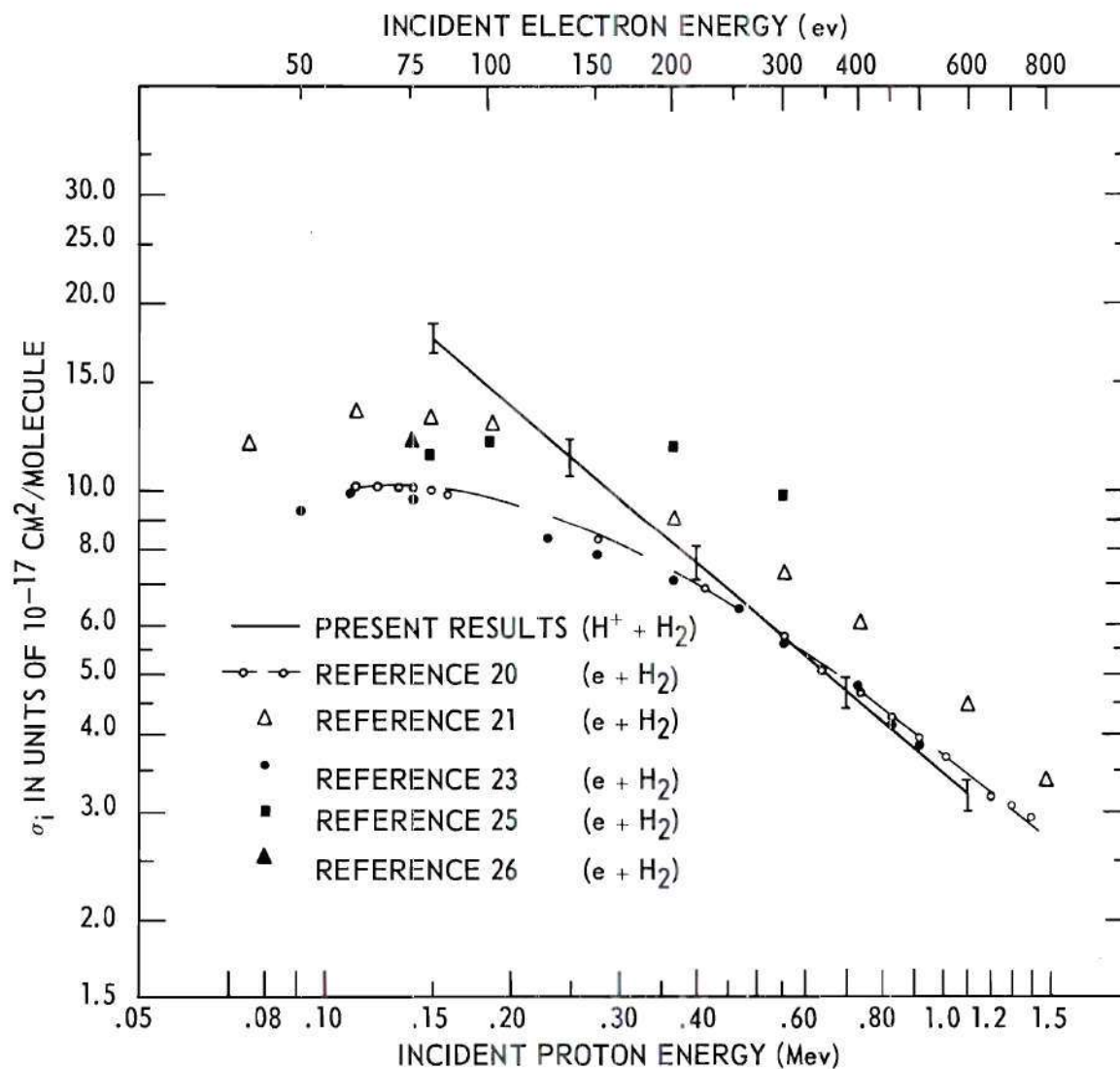


Figure 22. Comparison of Experimental Gross Ionization Cross Sections for Protons and Electrons of Equal Velocity Incident on Molecular Hydrogen.



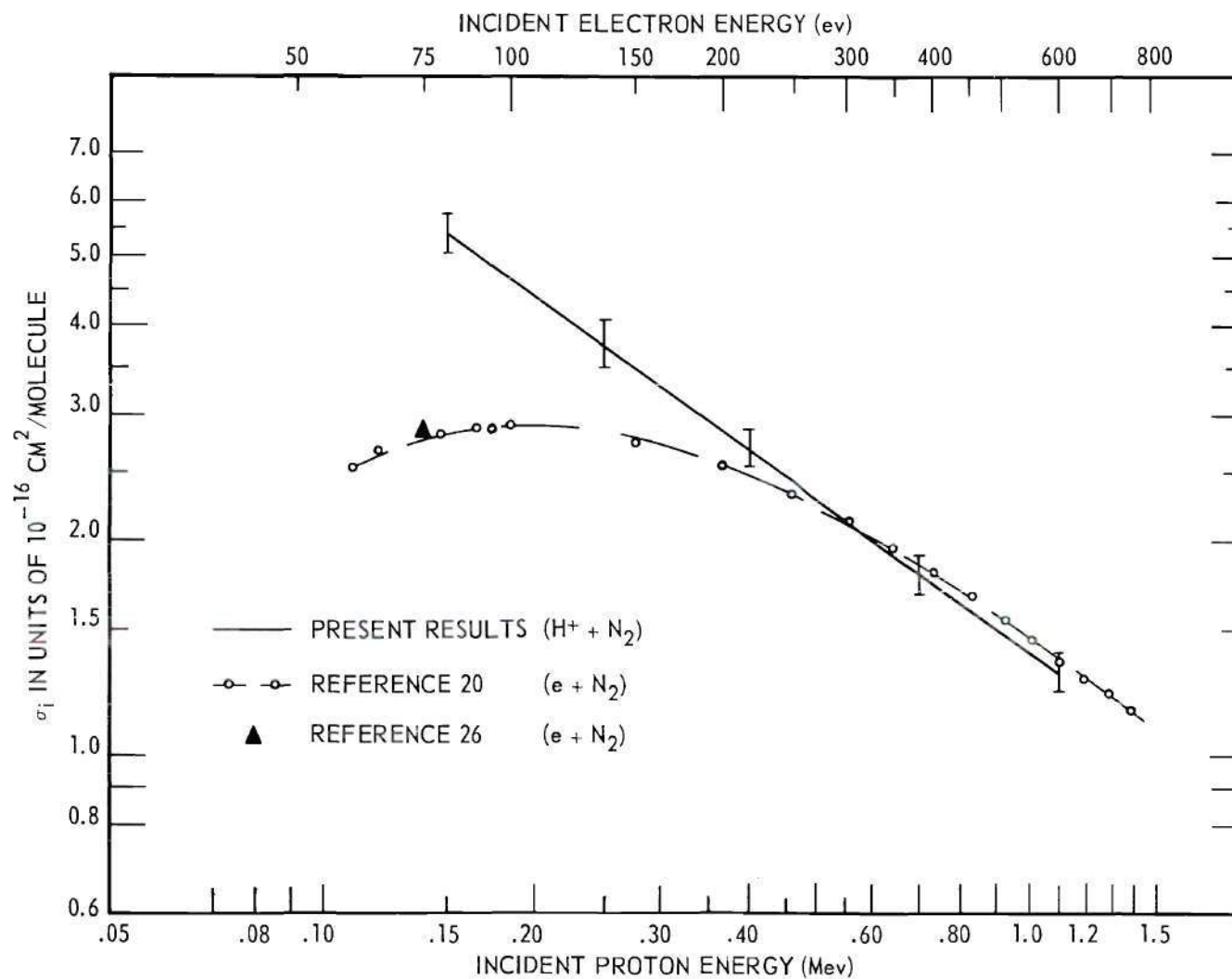


Figure 23. Comparison of Experimental Gross Ionization Cross Sections for Protons and Electrons of Equal Velocity Incident of Molecular Nitrogen.

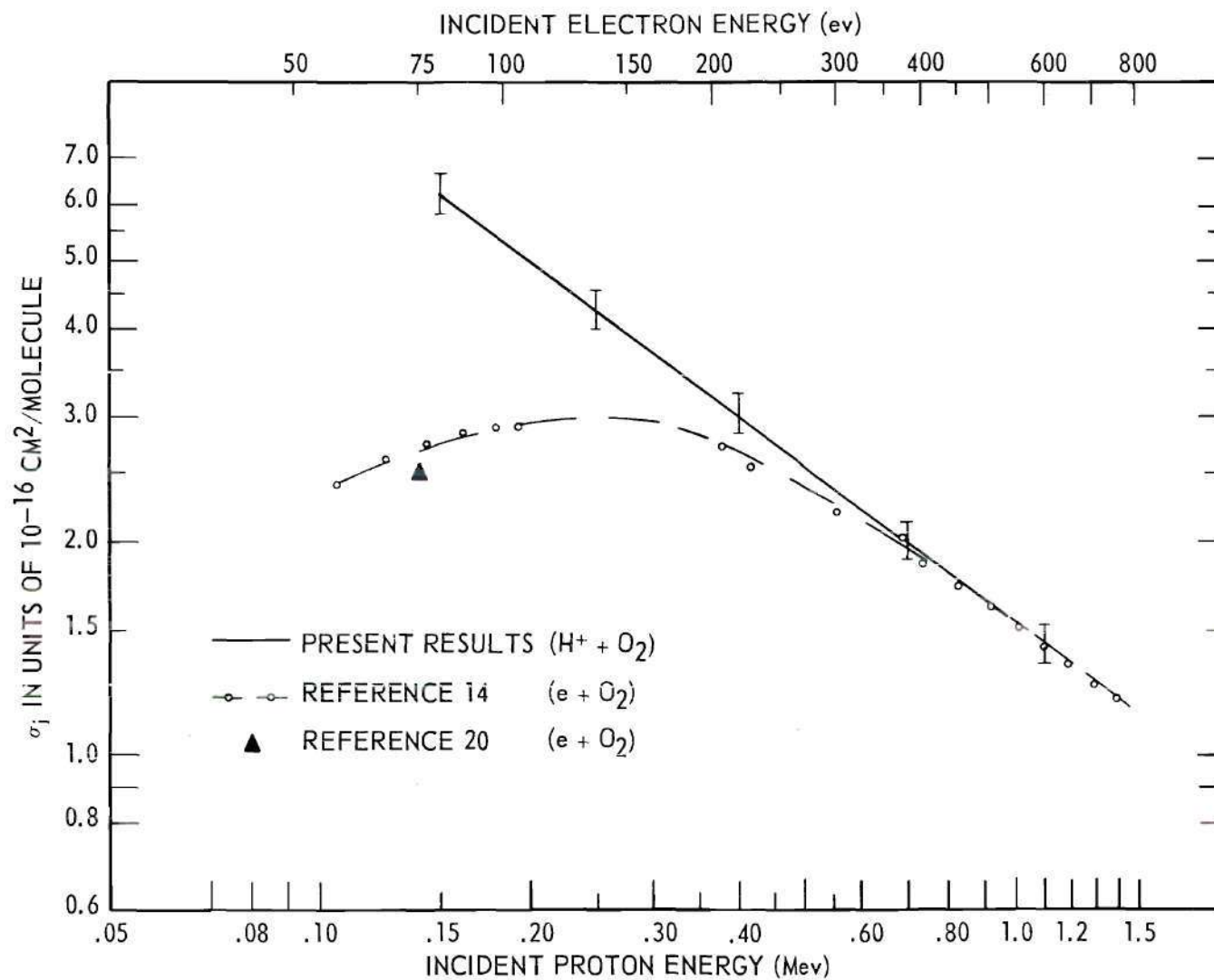


Figure 24. Comparison of Experimental Gross Ionization Cross Sections for Protons and Electrons of Equal Velocity Incident on Molecular Oxygen.

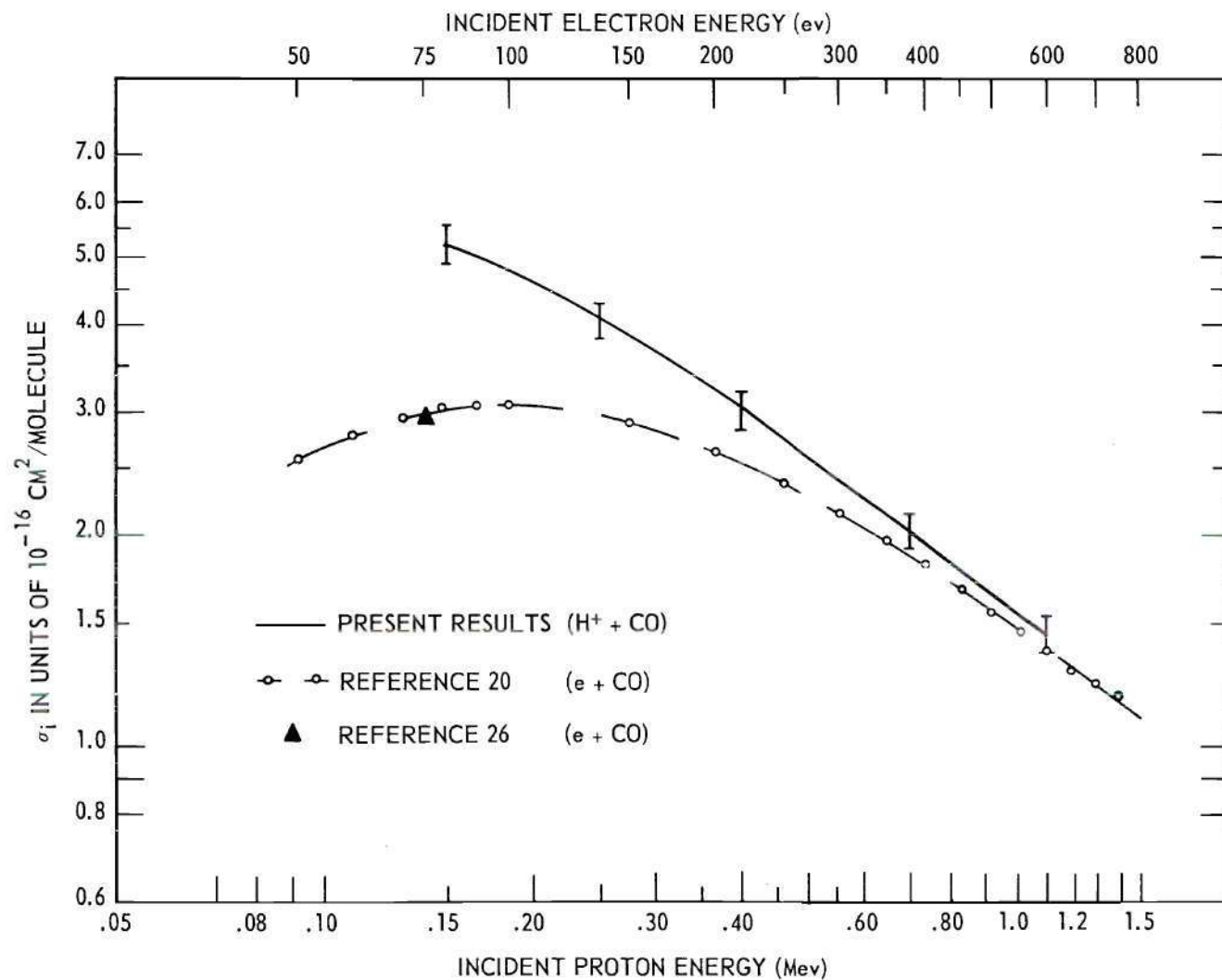


Figure 25. Comparison of Experimental Gross Ionization Cross Sections for Protons and Electrons of Equal Velocity Incident on Carbon Monoxide.

There is excellent agreement between the cross sections obtained with incident electrons and with incident protons of the same velocity for the target gases helium, neon, argon, nitrogen, oxygen, and carbon monoxide. There is also good agreement for the molecular hydrogen case if only the data of Tate and Smith<sup>20</sup>, Bleakney<sup>23</sup>, and Tozer and Craggs<sup>22</sup> are considered. The cross sections obtained by Harrison<sup>21</sup>, and by Compton and Van Voorhis<sup>25</sup> lie somewhat above the result obtained with incident protons. Harrison<sup>21</sup> has pointed out that the pressure measurements for his experiments were obtained with an ionization gauge whose calibration constant was 2.41. A constant of 3.20 would have led to results essentially identical to those of Tate and Smith.<sup>20</sup> Harrison's recalibration of his gauge yielded a constant of 2.50. The discrepancies therefore remain unresolved, however, the evidence seems to be in favor of the results of Tate and Smith.

An additional feature of comparison which is not apparent from Figures 23 and 25 is that according to the data of Tate and Smith the electron cross sections for nitrogen and carbon monoxide are equal at high energy whereas the proton results were found to be unequal by about 12 per cent. However, the electron results lie between the proton results for the two gases and are within the limits of the stated experimental uncertainties for the proton measurements on both gases. It does not seem likely that the proton experimental errors could be such as to lead to the observed displacement of the curves since, as it was pointed out in Chapter IV, the  $\pm 6$  per cent possible experimental error is believed to be largely systematic and attributable to inaccuracy in the McLeod gauge calibration.

The composite results indicate that it is justifiable to scale electron cross sections to proton cross sections for the gases investigated under the assumed high velocity conditions.



## CHAPTER VI

## CONCLUSIONS

The experimental values of the ionization cross sections for protons incident on helium, neon, argon, hydrogen, nitrogen, oxygen, and carbon monoxide are presented for comparison in Figure 26. The energy of the incident particles ranged from 0.15-1.10 Mev. Experimental points and limits-of-error flags are omitted to avoid unnecessary confusion. For all cases except carbon monoxide the results may be expressed throughout the energy range 0.15-1.10 Mev by an equation of the form  $\sigma_i = A \times E^{-C}$  cm<sup>2</sup>/molecule, where E is the incident proton energy in the laboratory coordinate system. Numerical values for the constants A and C, and their probable errors are given in Table I, Chapter IV.

A scaling of the theoretical calculation in the Born approximation of the cross section for the ionization of atomic hydrogen to the experimentally determined molecular results has been accomplished.<sup>1</sup> The scaled cross sections are in close agreement with experimental values at high energy. The validity of some of the assumptions made in the scaling process (e.g., that the difference between the electronic wave functions of the hydrogen molecule and those of the hydrogen atom can be neglected) is questionable; however, the results of such a scaling clearly indicate that the common practice of merely doubling the cross section for atomic cases to obtain the associated molecular results is suspect.

Born approximation calculations by Mapleton<sup>12</sup> for protons incident on helium targets have been found to be in excellent agreement with this

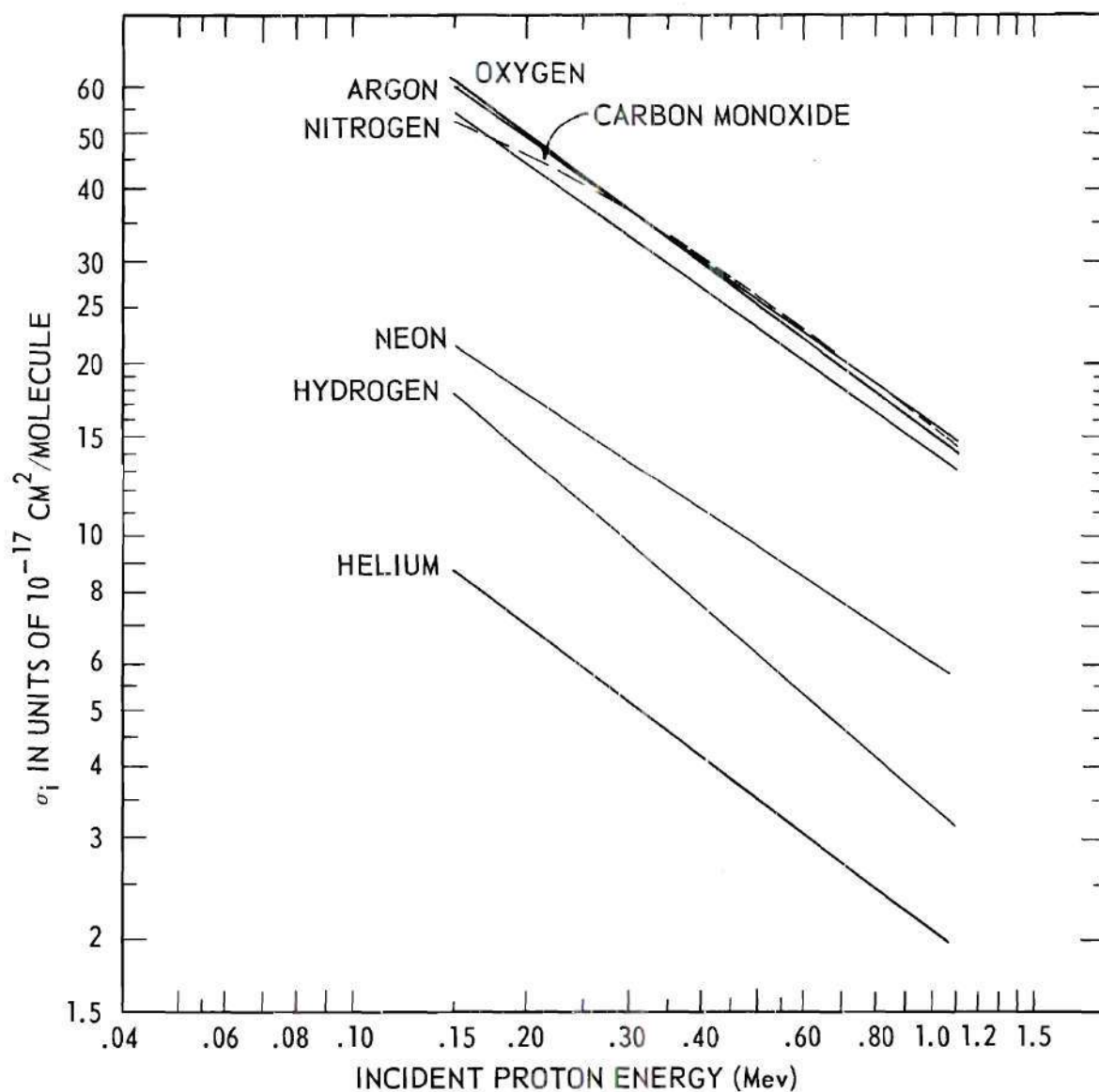


Figure 26. Gross Ionization Cross Sections for Protons Incident on Helium, Neon, Argon, Molecular Hydrogen, Molecular Nitrogen, Molecular Oxygen, and Carbon Monoxide.

experiment. Further corroboration of the experimental results for incident protons comes from a comparison of the scaled cross sections for  $\alpha$ -particles incident on helium which have been calculated by Erskine.<sup>17</sup>

It has been established that for sufficiently high, and equal, velocities of relative motion, the ionization cross sections for electrons and for protons incident on helium, neon, argon, hydrogen, nitrogen, oxygen, and carbon monoxide are the same within the limits of the estimated experimental error of this experiment.

## APPENDIX

## THE CONCEPT OF THE COLLISION CROSS SECTION

The various reactions which can occur when a beam of monoenergetic particles traverses a gas may be described in terms of reaction cross sections. The following development is only one of several possible presentations of the cross section concept.

Consider a monoenergetic beam of  $N_0$  particles per second incident upon a gas whose density is  $n$  particles per cubic centimeter. Let  $N(x)$  represent the incident beam particles which have not undergone a reaction in traversing the distance  $x$  in the gas. The change in the unreacted component of the beam in traversing an infinitesimal distance  $dx$  beyond the point  $P$  located  $x$  units within the gas will be proportional to  $N(x)$ ,  $n$ , and  $dx$ . Or:

$$- \frac{dN(x)}{dx} \sim N(x)n \quad (18)$$

where the minus sign indicates a decrease in the number of unreacted particles.

Let the constant of proportionality be represented by  $\sigma$ . Then:

$$- \frac{dN(x)}{dx} = \sigma N(x)n \quad (19)$$

Integration of equation (19) followed by evaluation of the arbitrary constant yields:

$$N(x) = N_0 e^{-n\sigma x} \quad (20)$$

A knowledge of  $N_0$ ,  $N(x)$ , and  $n$  leads to a determination of  $\sigma$ . It will be observed that the proportionality constant  $\sigma$  has the dimensions of (centimeters)<sup>2</sup>. Therefore  $\sigma$  is called the total reaction cross section for the specific target-projectile combination. It is sometimes convenient to consider the cross section to be an effective projected area of the target particle for the particular reaction or reactions of interest.

If the reactions of interest are those which arise in collision processes,  $\sigma$  may be considered to be the total collision cross section. This total collision cross section may be considered to be made up of the sum of the cross sections for elastic and inelastic collisions of all possible types. Thus:

$$\sigma = \sum \sigma_n \quad (21)$$

where  $\sigma_0$ ,  $\sigma_1$ ,  $\sigma_2$ ,  $\sigma_3$ , etc. represent the individual cross sections. In general  $\sigma$  and all of the  $\sigma_n$  are functions of the particle velocity.

To illustrate the use of the concept of collision cross section, consider the following experiment. A homogeneous ion beam is injected into a collision chamber containing target gas atoms at a pressure sufficiently low to insure that only single collisions will occur. It is evident that for ionizing collisions equal quantities of positive and negative charge will be produced in the collision region. Thus a gross ionization cross section for the production of free electrons can be determined by measurement of the ionization electron current.



To construct a model for this experiment let  $n$  represent the number of target atoms per unit volume,  $\sigma_1^-$  the cross section of each target structure for the production of electrons,  $A$  the cross sectional area of gas presented to the incident beam, and  $N_0$  the total number of incident particles per second. It follows from the earlier discussion that if we consider an element of the gas of thickness  $dx$  the fraction of the target area blocked by the target particles is:

$$f = \frac{A \sigma_1^- n dx}{A} = \sigma_1^- n dx \quad (22)$$

This result is based on the assumption that the gas pressure is sufficiently low to preclude any shielding of one target atom by another.

$N_0 \sigma_1^- n dx$  collisions will occur in the length  $dx$ . If a sufficiently small number of reactions occur to insure that the incident beam is essentially unaltered in passing through the collision region,  $N_0 \sigma_1^- n \ell$  collisions will occur in the total collision chamber length  $\ell$ . The application of a transverse electric field will result in the collection of a number of electrons which is proportional to the gross electron ionization cross section  $\sigma_1^-$ . The total number of electrons collected per unit time under the preceding conditions will be equal to  $N_0 \sigma_1^- n \ell$ . The collected electrons will produce a current  $I^-$  equal to  $N_0 \sigma_1^- n \ell e$ , where  $e$  denotes the electron charge.

All of the incident beam current  $I_1$  passes through the collision chamber and is collected. It follows that the ratio of the electron current to the total beam current is given by:

$$\frac{I^-}{I_i} = \frac{N_o e \sigma_i^- n \ell}{N_o e} = \sigma_i^- n \ell \quad (23)$$

Therefore the gross electron ionization cross section for this special case is:

$$\sigma_i^- = \left(\frac{1}{n \ell}\right) \left(\frac{I^-}{I_i}\right) \text{ cm}^2/\text{target particle} \quad (24)$$

A similar analysis applied to a measurement of residual positive ions would lead to the result:

$$\sigma_i^+ = \left(\frac{1}{n \ell}\right) \left(\frac{I^+}{I_i}\right) \text{ cm}^2/\text{target particle} \quad (25)$$

## BIBLIOGRAPHY

1. Bates, D. R. and G. Griffing, "Inelastic Collisions Between Heavy Particles I: Excitation and Ionization of Hydrogen Atoms in Fast Encounters with Protons and with Other Hydrogen Atoms," Proceedings of the Physical Society (London), A 66, 961 (1953).
2. Mapleton, R. A., "Simultaneous Ionization and Excitation of Helium by Protons," Physical Review, 109, 1166 (1958).
3. McDowell, M. R. C. and G. Peach, "Ionization of Lithium by Fast Protons and Electrons," Physical Review, 121, 1383 (1961).
4. Barnett, C. F. and H. K. Reynolds, "Charge Exchange Cross Sections of Hydrogen Particles in Gases at High Energies," Physical Review, 109, 355 (1958).
5. Massey, H. S. W. and E. H. S. Burhop, Electronic and Ionic Impact Phenomena, London: Oxford University Press, 1956.
6. Afrosimov, V. V., Il'in, R. N. and N. V. Fedorenko, "Ionization of Molecular Hydrogen by  $H^+$ ,  $H_2^+$ , and  $H_3^+$  Ions," Soviet Physics-Journal of Experimental and Theoretical Physics, 34, 968 (1958).
7. Fedorenko, N. V., Afrosimov, V. V., Il'in, R. N. and E. S. Solov'ev, "Ionization of Inert Gases by Protons," appearing in Ionization Phenomena in Gases, Edited by N. R. Nilsson, Amsterdam: North Holland Publishing Company, 1960, p. IA 47.
8. Allison, S. K., "Charge-Changing Collisions of Hydrogen and Helium Atoms and Ions at Kinetic Energies Above 0.2 kev," Reviews of Modern Physics, 30, 1137 (1958).
9. Allison, S. K. and M. Garcia-Munoz, "Electron Capture and Loss at High Energies," appearing in Atomic and Molecular Processes, Edited by D. R. Bates, New York: Academic Press, Inc. (In Press).
10. Hasted, J. B., "Inelastic Collisions Between Atomic Systems," appearing in Advances in Electronics and Electron Physics, 13, New York: Academic Press, Inc., 1960.
11. Stier, P. M. and C. F. Barnett, "Charge Exchange Cross Sections for Helium Ions in Gases," Physical Review, 109, 385 (1958).
12. Keene, J. P., "Ionization and Charge Exchange by Fast Ions of Hydrogen and Helium," Philosophical Magazine, 40, 369 (1949).



13. Stedeford, J. B. H. II and J. B. Hasted, "I: Further Investigations of Charge Exchange and Electron Detachment. Ion Energies 3-40 kev. II: Ion Energies 100-4000 ev.," Proceedings of the Royal Society (London), A 227, 466 (1955).
14. Gilbody, H. B. and J. B. Hasted, "Ionization by Positive Ions," Proceedings of the Royal Society, A 240, 382 (1957).
15. Fogel, Ia. M., Kruprik, L. I. and B. G. Safronov, "Capture of Electrons and Ionization by Protons in Hydrogen," Soviet Physics-Journal of Experimental and Theoretical Physics, 1, 415 (1955).
16. Schwirzke, F., "Ionisierungs- und Umladequerschnitte von Wasserstoff-Atomen und Ionen von 9 bis 60 kev in Wasserstoff," Zeitschrift für Physik, 157, 510 (1960).
17. Erskine, G. A., "Calculation of the Energy per Ion Pair for  $\alpha$ -Particles in Helium," Proceedings of the Royal Society (London), A 224, 362 (1954).
18. Smith, P. T., "The Ionization of Helium, Neon, and Argon by Electron Impact," Physical Review, 36, 1293 (1930).
19. Mott, N. F. and H. S. W. Massey, The Theory of Atomic Collisions, 2nd ed. London: Oxford University Press, 1949, p. 271.
20. Tate, J. T. and P. T. Smith, "The Efficiencies of Ionization and Ionization Potentials of Various Gases under Electron Impact," Physical Review, 39, 270 (1932).
21. Harrison, H., The Experimental Determination of Ionization Cross Sections of Gases under Electron Impact, Washington: Catholic University Press, 1956.
22. Tozer, B. A. and J. D. Craggs, "Cross Sections for Ionization of the Inert Gases by Electron Impact," Journal of Electronics and Control, 8, 103 (1960).
23. Bleakney, W., "The Ionization of Hydrogen by Single Electron Impact," Physical Review, 35, 1180 (1930).
24. Bleakney, W., "Ionization Potentials and Probabilities for the Formation of Multiply Charged Ions in Helium, Neon, and Argon," Physical Review, 36, 1303 (1930).
25. Compton, K. T. and C. C. Van Voorhis, "Ionization of Gas Molecules by Electron Impacts," Physical Review, 26, 436 (1925).
26. Lampe, F. W., Franklin, J. L. and F. H. Field, "Cross Sections for Ionization by Electrons," Journal of the American Chemical Society, 79, 6129 (1957).

## VITA

John William Hooper was born in Hazen, Arkansas, on June 9, 1931. He is the son of John Word and Caroline Kesler Hooper. In September of 1957 he was married to Mary Anne Wachal of Hazen, Arkansas.

He attended public school in Hazen, Arkansas, and was graduated in 1949. He received the degrees of Bachelor of Science in Electrical Engineering and Bachelor of Science in Business Administration from Kansas State College in January, 1954. He was awarded the degree Master of Science in Electrical Engineering by the Georgia Institute of Technology in 1955.

Following a brief period of employment with the General Electric Company, he served two years with the Army Ballistic Missile Agency and the Guided Missile Development Division of the United States Army.

He returned to the Georgia Institute of Technology in 1957 as a graduate assistant. In 1958-59 he served as an Instructor of Electrical Engineering. Since 1959 he has been an Instructor of Electrical Engineering and Research Associate at the Engineering Experiment Station.